INTERNATIONAL JOURNAL OF ROBUST AND NONLINEAR CONTROL
Int. J. Robust Nonlinear Control 2017; **27**:781–803
Published online 10 August 2016 in Wiley Online Library (wileyonlinelibrary.com). DOI: 10.1002/rnc.3600

Consensus and disturbance attenuation in multi-agent chains with nonlinear control and time delays

Linjun Zhang*,† and Gábor Orosz

Department of Mechanical Engineering, University of Michigan, Ann Arbor, MI 48105, USA

SUMMARY

In this paper, we investigate consensus and disturbance attenuation in a chain of mobile agents, which include non-autonomous agents, semi-autonomous agents and autonomous agents. In particular, the nonlinear dynamics of non-autonomous agents is given and cannot be designed, while the dynamics of semi-autonomous and autonomous agents can be partially and fully designed, respectively. To improve the robustness of multi-agent chains against disturbances, we propose a nonlinear control framework for semi-autonomous and autonomous agents such that they mimic the behavior of non-autonomous agents for compatibility while also exploiting long-range connections with distant agents. This framework ensures the existence of a unique consensus equilibrium, which is independent of the network size, connectivity topologies, control gains and information delays. Robustness of multi-agent chains against disturbances is investigated by evaluating the frequency response at the nonlinear level. For infinitely long multi-agent chains with recurrent patterns, we also derive a condition that ensures the disturbance attenuation but only requires the analysis of the linearized model. A case study is conducted for a connected vehicle system where numerical simulations are used to validate the analytical results. Copyright © 2016 John Wiley & Sons, Ltd.

Received 23 December 2015; Revised 18 April 2016; Accepted 15 June 2016

KEY WORDS: multi-agent chains; nonlinear systems; time delays; consensus; disturbance attenuation

1. INTRODUCTION

Distributed control for cooperation in multi-agent networks has been attracting an increasing attention in recent years. This is due to its broad range of applications such as systems biology [1], distributed sensor networks [2] and connected vehicle systems [3–5]. One fundamental design objective of multi-agent networks is to achieve consensus, which requires all agents to maintain desired relative states with respect to their neighbors [6]. In [7], consensus in directed networks with switching topologies and time delays was investigated. In [8], the authors developed a linear iteration that yields distributed averaging consensus over a network. Network consensus with state constraints was investigated in [9], while [10] focused on the input–output property of a linear networked system with communication delays. For directed networks with nonlinear dynamics, consensus was studied in [11] by local consensus manifold approach and by Lyapunov methods. In [12], the effects of nonlinear dynamics and sampling delays on consensus were investigated. The event-triggered sampled-data consensus problem was studied in [13].

When studying network consensus, external disturbances are typically neglected. However, disturbances are inevitable in physical systems, and they may propagate through the network and jeopardize the consensus by causing oscillations or even divergence. For instance, a slight deceleration of a vehicle in traffic may lead to stop-and-go motion of vehicles further upstream when the

*Correspondence to: Linjun Zhang, Department of Mechanical Engineering, University of Michigan, Ann Arbor, MI 48105, USA.
†E-mail: linjunzh@umich.edu

disturbance is amplified while propagating along the chain of vehicles [14, 15]. Disturbance attenuation in undirected networks of agents with identical linear dynamics was investigated in [16], while a distributed $\mathcal{H}_\infty$ control for network consensus was presented in [17]. For chains of connected and automated vehicles (CAVs), disturbance attenuation is often called 'string stability' and has been widely studied [18–25].

The aforementioned studies on disturbance attenuation in networks assumed that the dynamics of all agents can be designed. However, in practice, there may exist non-autonomous agents (NAAs) that follow certain rules based on their own perception so that their dynamics cannot be designed. On the other hand, the dynamics of semi-autonomous (SAAs) and autonomous (AAs) agents may be partially and fully designed, respectively, while they may also exploit long-range interactions with distant agents. For example, this occurs in connected vehicle systems where human-driven vehicles are mixed with vehicles of higher levels of autonomy that can exploit wireless vehicle-to-vehicle communication [3]. Similar phenomena can be found when attaching controller genes to gene regulatory networks [26] and when controlling neural ensembles using brain–machine interfaces [27]. In nature, the dynamics of NAAs is often nonlinear. For compatibility, it is crucial to ensure that the SAAs and AAs follow similar rules as the NAAs. Thus, their controllers need to be nonlinear as well. Moreover, time delays often arise in the information exchange between agents. Distributed nonlinear control for consensus and disturbance attenuation in time-delayed networks that include NAAs is still an open problem.

In this paper, we focus on a class of multi-agent chains where NAAs only respond to the motion of the nearest agent, while SAAs and AAs may also respond to the motion of multiple distant agents. We propose a nonlinear control framework for SAAs and AAs, which ensures the existence of a unique consensus equilibrium independent of the network size, connectivity topologies, control gains and information delays. Then, we provide a condition that ensures that each SAA and AA can approach the consensus equilibrium when no disturbances arise from other agents. Robustness of multi-agent chains against disturbances is studied by evaluating the frequency response at the nonlinear level. In particular, the steady state is analytically approximated for nonlinear time-delayed chains and such closed-form solution remains scalable for large networks. For infinitely long chains with recurrent patterns, we also provide a condition that ensures disturbance attenuation by only requiring the analysis of the corresponding linearized model. This significantly reduces the complexity of design and analysis.

The rest of this paper is organized as follows. In Section 2, we present the nonlinear control framework for the SAAs and AAs, and we also provide the definitions for consensus and disturbance attenuation. In Sections 3 and 4, we present conditions for consensus and disturbance attenuation in multi-agent chains, respectively. A case study is conducted in Section 5 by applying the presented theorems to connected vehicle systems. In Section 6, we conclude our results and discuss future research directions.

2. PROBLEM FORMULATION

In this section, we introduce a framework for the dynamics of multi-agent chains that include NAAs, SAAs and AAs. Then, consensus and disturbance attenuation in such systems are defined.

2.1. Multi-agent chains

Here, we consider a chain of mobile agents in one spatial dimension where each agent may monitor the motion of multiple agents ahead. For example, in Figure 1, agent i monitors the positions s_j and the velocities v_j of agents j for $j = i-1, \ldots, p_i$, where p_i represents the furthest agent within the communication range of agent i. The length of agent j is denoted by l_j, while the symbol $\xi_{i,j}$ denotes the time delay for information exchange between agents i and j. Note that some agents may not broadcast information; see agent $i-2$ in Figure 1.

We define the state and the output of agent i as

$$x_i(t) = \begin{bmatrix} s_i(t) \\ v_i(t) \end{bmatrix}, \quad y_i(t) = v_i(t) \tag{1}$$

DOI: 10.1002/rnc

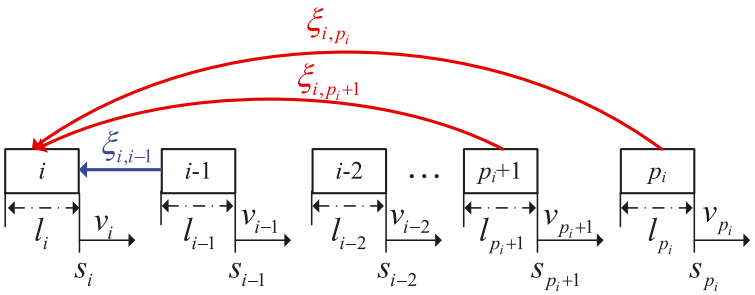

Figure 1. A multi-agent chain where an agent monitors the motion of multiple agents ahead. The short-range link (blue) can be realized by range sensors (e.g. human perception, radar and lidar) or wireless communication, while the long-range links (red) can only be realized by wireless communication as distant agents are beyond the line of sight. Symbols s_j, l_j and v_j denote the position, length and velocity of agent j, respectively. The information delays between agents i and j are denoted by $\xi_{i,j}$ for $j = i-1, \dots, p_i$.

and assume that the acceleration of agent i is directly given by the control input $u_i(t)$ so that its dynamics is governed by a second-order integrator

$$\begin{aligned} \dot{x}_i(t) &= \begin{bmatrix} 0 & 1 \\ 0 & 0 \end{bmatrix} x_i(t) + \begin{bmatrix} 0 \\ 1 \end{bmatrix} u_i(t)\,, \\ y_i(t) &= \begin{bmatrix} 0 & 1 \end{bmatrix} x_i(t)\,. \end{aligned} \tag{2}$$

Although the dynamic model (2) is linear, the closed-loop dynamics becomes nonlinear when the control input u_i is a nonlinear function of the state x_i. Moreover, the control input u_i may bring information delays into the system.

Considering that a multi-agent chain may contain agents of different levels of autonomy, we define three types of agents as follows.

- *Non-autonomous agent* only monitors the motion of the agent immediately ahead. Its controller is predetermined and cannot be designed.
- *Semi-autonomous agent* responds to the agent immediately ahead with predetermined dynamics and also responds to distant agents using a controller that can be designed to exploit long-range interactions.
- *Autonomous agent* responds to multiple agents ahead, and the corresponding controller can be fully designed.

In connected vehicle systems, these three types of agents represent human-driven vehicles, vehicles with advanced driver assistance systems and fully automated vehicles, respectively. In human–robot interactive systems, NAAs and AAs represent human and robots, respectively, while SAAs represent humans equipped with assistance devices (e.g. exoskeletons). The first agent in the chain may follow a given trajectory instead of responding to other agents. Thus, it can be any of these three types of agents.

We assume that each NAA determines its acceleration based on its distance and relative speed to the agent immediately ahead, aiming to maintain the desired distance and speed. To achieve this goal, we assume the control law of a NAA k in the form

$$\begin{aligned} u_k(t) = \alpha_{k,k-1} \left(V\left(h_{k,k-1}(t-\xi_{k,k-1})\right) - v_k(t-\xi_{k,k-1}) \right) \\ + \beta_{k,k-1} \left(v_{k-1}(t-\xi_{k,k-1}) - v_k(t-\xi_{k,k-1}) \right)\,, \end{aligned} \tag{3}$$

where $\alpha_{k,k-1}$ and $\beta_{k,k-1}$ are constant gains, while the distance between agents k and $k-1$ is

$$h_{k,k-1}(t) = s_{k-1}(t) - s_k(t) - l_{k-1}\,, \tag{4}$$

see Figure 1. The function $V(h)$ is used to determine the desired velocity based on the distance and can be written in the form

DOI: 10.1002/rnc

$$V(h) = \begin{cases} 0\,, & \text{if } h \leqslant h_{\text{st}}\,, \\ F(h)\,, & \text{if } h_{\text{st}} < h < h_{\text{go}}\,, \\ v_{\max}\,, & \text{if } h \geqslant h_{\text{go}}\,, \end{cases} \tag{5}$$

where h_{st}, h_{go} and $v_{\max}$ are positive constants. This means that the agent tends to stop for small distances $h \leqslant h_{\text{st}}$ while aiming to maintain the preset maximum speed $v_{\max}$ for large distances $h \geqslant h_{\text{go}}$. For $h_{\text{st}} < h < h_{\text{go}}$, the desired velocity is determined by the monotonically increasing nonlinear function $F(h)$ such that $V(h)$ is continuously differentiable at $h = h_{\text{st}}$ and $h = h_{\text{go}}$, which cannot be achieved by linear functions. For the subsequent control design, we assume that for NAAs, the control law (3) and the control gains $\alpha_{k,k-1}$, $\beta_{k,k-1}$ are known but cannot be modified. In practice, these parameters may be estimated by using system identification.

For compatibility, it is desired that SAAs and AAs can mimic the behavior of NAAs. Thus, considering the NAAs' control strategy (3), we present a control framework for SAAs and AAs. For the controller of agent i, we propose

$$u_i(t) = \sum_{j=p_i}^{i-1} \left[\alpha_{i,j}\left(V\left(h_{i,j}(t-\xi_{i,j})\right) - v_i(t-\xi_{i,j})\right) + \beta_{i,j}\left(v_j(t-\xi_{i,j}) - v_i(t-\xi_{i,j})\right)\right], \tag{6}$$

for $i = 1, \ldots, n$, where the function $V(h)$ is given in (5) and the quantity

$$h_{i,j}(t) = \frac{s_j(t) - s_i(t) - \sum_{k=j}^{i-1} l_k}{i-j} \tag{7}$$

denotes the average distance between agents i and j for $j = p_i, \ldots, i-1$. Such averaging is used to make the desired velocity $V(h_{i,j})$ comparable for different j's. In (6), the constants

$$\alpha_{i,j} = \gamma_{i,j}\overline{\alpha}_{i,j}\,, \quad \beta_{i,j} = \gamma_{i,j}\overline{\beta}_{i,j} \tag{8}$$

denote the effective control gains along the link from agent j to agent i, where $\overline{\alpha}_{i,j}, \overline{\beta}_{i,j}$ are the actual control gains, while $\gamma_{i,j}$ is determined by the connectivity topology such that

$$\gamma_{i,j} = \begin{cases} 1\,, \text{if agent } i \text{ uses the data of agent } j\,, \\ 0\,, \text{otherwise}\,. \end{cases} \tag{9}$$

Note that, in multi-agent chains, every agent must respond to the agent immediately ahead for safety reasons. Thus, $\gamma_{i,i-1} = 1$ always holds. We also remark that, for SAA i, the gains $\alpha_{i,i-1}$ and $\beta_{i,i-1}$ are known but cannot be modified ,while the gains $\alpha_{i,j}$ and $\beta_{i,j}$ for $j < i-1$ can be designed. For AAs, all gains can be designed.

2.2. *Consensus and disturbance attenuation*

Consensus and disturbance attenuation are two crucial properties of multi-agent networks. For a chain of mobile agents, consensus implies that each pair of consecutive agents maintain a constant distance while moving at the same speed. For simplicity, we assume identical distance h^*, that is,

$$x_{j-1}(t) - x_j(t) \equiv \begin{bmatrix} h^* \\ 0 \end{bmatrix}, \tag{10}$$

for all $j = 1, 2, \ldots$ (cf. (1)). Thus, when the leading agent moves at a constant speed v^*, the equilibrium for consensus (10) can be described by

$$x_j^*(t) = \begin{bmatrix} s_j^*(t) \\ v^* \end{bmatrix}, \tag{11}$$

where $s_j^*(t) = v^* t + \overline{s}_j$ and $\overline{s}_{j-1} - \overline{s}_j - l_{j-1} = h^*$.

DOI: 10.1002/rnc

Definition 1
A multi-agent chain is said to *approach consensus* if and only if

$$x_j(t) \to x_j^*(t)\,, \quad \text{as } t \to \infty \text{ for } j = 1, 2, \ldots \tag{12}$$

(cf. (1) and (11)).

For NAAs (2) and (3), at consensus, the desired distance h^* and the desired speed v^* satisfy the range policy (5)

$$v^* = V(h^*)\,. \tag{13}$$

Typically, consensus (12) may be achieved in the absence of external disturbances. However, in practice, disturbances may arise from some agents and propagate to other agents. This may jeopardize consensus if disturbances are amplified when propagating along the chain. We define the perturbation about the consensus equilibrium (11) as

$$\tilde{x}_i(t) = x_i(t) - x_i^*(t)\,, \qquad \tilde{y}_i(t) = y_i(t) - y_i^*(t)\,, \tag{14}$$

where $y_i^*(t) \equiv v^*$ (cf. (1) and (11)). In an $(n+1)$-agent chain, the perturbation arising from the head agent 0 propagates along all other agents and eventually reaches the tail agent n.

Definition 2
Considering the output of the head agent $y_0(t)$ as the input for the chain and the output of the tail agent $y_n(t)$ as the output for the chain, we say that the chain is capable of *input–output disturbance attenuation* in the $\mathcal{L}_p$ norm if and only if

$$\|\tilde{y}_n^{(\mathrm{s})}\|_{\mathcal{L}_p} < \|\tilde{y}_0^{(\mathrm{s})}\|_{\mathcal{L}_p}\,, \tag{15}$$

where the superscript (s) represents the steady state and $p = 1, 2, \ldots$.

Here, we use the steady state to evaluate the disturbance attenuation to make the results independent of the initial conditions. Note that (15) depends on the choice of norms and, thus, one may obtain different conclusions about disturbance attenuation for the same network by using different norms. To bypass this problem, one may construct an infinitely long chain by cascading the original network such that the tail agent of a block becomes the leading agent of another block; see Figure 2. In the cascading chain, the tail agent of the k-th block is indexed by kn. For such cascade, (15) may not imply $\|\tilde{y}_{kn}^{(\mathrm{s})}\|_{\mathcal{L}_p} < \|\tilde{y}_{(k-1)n}^{(\mathrm{s})}\|_{\mathcal{L}_p}$ for all $k = 1, 2, \ldots$ due to the nonlinear dynamics.

Definition 3
A multi-agent chain is said to be capable of *eventual disturbance attenuation* if and only if the disturbances decay to zero in the corresponding cascade, that is,

$$\tilde{x}_{kn}(t) \to 0\,, \quad \text{as } t \to \infty\,, k \to \infty\,. \tag{16}$$

Note that Definitions 2 and 3 both allow disturbances to be amplified by some agents in the network. Such flexibility is useful for networks containing NAAs, for which the dynamics cannot be designed. Indeed, Definitions 2 and 3 are independent of each other and describe the disturbance attenuation from different aspects. The input–output disturbance attenuation (15) evaluates whether the disturbance imposed on the head agent can be attenuated when reaching the tail agent in a given network, while the eventual disturbance attenuation (16) evaluates whether the disturbance can be eliminated in an infinitely long chain with recurrent connectivity topology.

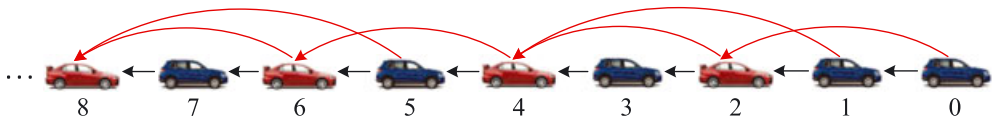

Figure 2. A connected vehicle system with recurrent connectivity topology; compare agents 0–4 and 4–8.

DOI: 10.1002/rnc

3. CONSENSUS IN MULTI-AGENT CHAINS

In this section, we study the consensus of multi-agent chains (2) with the distributed controller (6). First, we provide a sufficient condition that ensures the existence of a unique consensus equilibrium.

Theorem 1
If the control gains $\overline{\alpha}_{i,j}$ are positive for $i, j = 1, \ldots, n$ in (8) and $v_0(t) \equiv v^*$ with $0 < v^* < v_{\max}$, the control framework (6) guarantees the existence of a unique consensus equilibrium (11) that satisfies (10) and (13) and is independent of the network size, connectivity topologies, control gains and information delays.

The proof is presented in Appendix A. The control framework (6) ensures the uniqueness and the independence of the consensus equilibrium because we use the average distance (7) while also exploiting the identical range policy $V(h)$ for each link. Theorem 1 is crucial for ensuring the desired performance of multi-agent chains with complex connectivity topologies and information delays. Now, we further investigate how to design the control gains $\alpha_{i,j}$ and $\beta_{i,j}$ such that each agent can reach the consensus equilibrium.

Substituting (6), (11) and (13) into (2) and subtracting the corresponding model at consensus, we obtain

$$\begin{aligned}
&\dot{\tilde{s}}_i(t) = \tilde{v}_i(t)\,,\\
&\dot{\tilde{v}}_i(t) = \sum_{j=p_i}^{i-1} \left[\alpha_{i,j}\left(V\left(h_{i,j}(t-\xi_{i,j})\right) - V(h^*) - \tilde{v}_i(t-\xi_{i,j})\right) + \beta_{i,j}\left(\tilde{v}_j(t-\xi_{i,j}) - \tilde{v}_i(t-\xi_{i,j})\right)\right],
\end{aligned} \tag{17}$$

where $h_{i,j}$ is given in (7) (cf. (1) and (14)). In practice, it is often desired to maintain the distance and the velocity in invariant domains, that is,

$$h_{k,k-1}(t) \in \mathcal{D}_h \triangleq \{h : \underline{h} \leqslant h \leqslant \overline{h}\}\,, \quad \text{and} \quad v_k(t) \in \mathcal{D}_v \triangleq \{v : \underline{v} \leqslant v \leqslant \overline{v}\}\,, \tag{18}$$

for all $t \geqslant 0$ and $k = 1, \ldots, n$, where positive constants $\underline{h}$, $\overline{h}$, $\underline{v}$ and $\overline{v}$ are given bounds. In terms of the range policy (5), we assume $h_{\rm st} < \underline{h} < \overline{h} < h_{\rm go}$ and $0 < \underline{v} < \overline{v} < v_{\max}$. It follows that $h_{i,j}(t), h^* \in \mathcal{D}_h$ for $i, j = 1, \ldots, n$ and $v^* \in \mathcal{D}_v$ (cf. (7)). Because $V(h)$ is continuously differentiable, based on the mean value theorem [28], there exist variables $\psi_{i,j} \in \mathcal{D}_h$ such that

$$V(h_{i,j}(t)) - V(h^*) = V'(\psi_{i,j})\left(h_{i,j}(t) - h^*\right) = \frac{V'(\psi_{i,j})}{i-j}\left(\tilde{s}_j(t) - \tilde{s}_i(t)\right)\,, \tag{19}$$

(cf. (7)). We remark that the expression of $\psi_{i,j}$ is unique if $V'(h)$ is invertible for $\forall h \in \mathcal{D}_h$, while the value of $\psi_{i,j}$ exists but may be not unique if $V'(h)$ is not invertible. Note that $\psi_{i,j} = h^*$ when $h_{i,j}(t) = h^*$. In the subsequent analysis, we only need the existence of $\psi_{i,j}$.

Substituting (19) into (17) and writing the result in the matrix form, we obtain

$$\dot{\tilde{x}}_i(t) = A_{i,0}\,\tilde{x}_i(t) + \sum_{j=p_i}^{i-1}\left(A_{i,j}(\psi_{i,j})\,\tilde{x}_i(t-\xi_{i,j}) + B_{i,j}(\psi_{i,j})\,\tilde{x}_j(t-\xi_{i,j})\right)\,, \tag{20}$$

where $\tilde{x}_i(t)$ is given in (14) and the matrices are defined as

$$A_{i,0} = \begin{bmatrix} 0 & 1 \\ 0 & 0 \end{bmatrix}\,, \quad A_{i,j}(\psi_{i,j}) = \begin{bmatrix} 0 & 0 \\ -\varphi_{i,j}(\psi_{i,j}) & -\kappa_{i,j} \end{bmatrix}\,, \quad B_{i,j}(\psi_{i,j}) = \begin{bmatrix} 0 & 0 \\ \varphi_{i,j}(\psi_{i,j}) & \beta_{i,j} \end{bmatrix}, \tag{21}$$

for $j = p_i, \ldots, i-1$, where

$$\varphi_{i,j}(\psi_{i,j}) = \frac{\alpha_{i,j}V'(\psi_{i,j})}{i-j}\,, \qquad \kappa_{i,j} = \alpha_{i,j} + \beta_{i,j}\,. \tag{22}$$

DOI: 10.1002/rnc

Note that model (20) is indeed nonlinear because the matrices $A_{i,j}(\psi_{i,j})$ and $B_{i,j}(\psi_{i,j})$ depend on the states $h_{i,j}$ nonlinearly (cf. (19)).

One common method to ensure consensus in nonlinear time-delayed networks is to construct a Lyapunov functional for the whole network, which is challenging especially when the network contains a large number of agents. Here, we simplify the analysis by exploiting the property of the chain topology, that is, adding an agent at the tail does not affect the dynamics of agents ahead. This allows one to achieve chain consensus sequentially by ensuring that the newly added agent can approach the consensus equilibrium. That is, when studying agent i, we assume that all agents ahead have reached the consensus equilibrium, that is, $\tilde{x}_j(t) \equiv 0$ for $j = p_i, \ldots, i-1$. Considering this in (20) yields

$$\dot{\tilde{x}}_i(t) = A_{i,0}\,\tilde{x}_i(t) + \sum_{j=p_i}^{i-1} A_{i,j}(\psi_{i,j})\,\tilde{x}_i(t-\xi_{i,j})\,. \tag{23}$$

Note that in (23), the delays between different pairs of agents may have the same value. To eliminate such redundancy, we define an ordered set that only contains different values of delays

$$\sigma_i \triangleq \{\sigma_{i,0}, \sigma_{i,1}, \ldots, \sigma_{i,m_i}\}\,, \tag{24}$$

where $\sigma_{i,0} = 0$, $m_i \leqslant i - p_i$ and $\sigma_{i,k} < \sigma_{i,\ell}$ for $k < \ell$ such that the set σ_i is equivalent to the set $\{0, \xi_{i,p_i}, \ldots, \xi_{i,i-1}\}$. Here, we include element 0 in σ_i to make the subsequent expressions more compact. Then, one can collect the terms with the same delay values and obtain

$$\dot{\tilde{x}}_i(t) = \sum_{k=0}^{m_i} \hat{A}_{i,k}(\Psi_i)\,\tilde{x}_i(t-\sigma_{i,k})\,, \tag{25}$$

where $\Psi_i = [\psi_{i,i-1}, \ldots, \psi_{i,p_i}] \in \mathcal{D}_h^{i-p_i}$ and the superscript $i - p_i$ refers to the direct product of $\mathcal{D}_h$ by $i - p_i$ times. Note that (23) and (25) are equivalent but describe the system from different aspects: (23) highlights the connectivity topology, while (25) emphasizes different information delays.

Based on the Newton–Leibniz formula, we have the identity

$$\tilde{x}_i(t-\sigma_{i,k}) = \tilde{x}_i(t) - \int_{t-\sigma_{i,k}}^{t} \dot{\tilde{x}}_i(\tau)\,\mathrm{d}\tau = \tilde{x}_i(t) - \sum_{\ell=1}^{k} \int_{t-\sigma_{i,\ell}}^{t-\sigma_{i,\ell-1}} \dot{\tilde{x}}_i(\tau)\,\mathrm{d}\tau\,. \tag{26}$$

Substituting (26) into (25) results in

$$\dot{\tilde{x}}_i(t) = \overline{A}_{i,0}(\Psi_i)\,\tilde{x}_i(t) - \sum_{q=1}^{m_i} \overline{A}_{i,q}(\Psi_i) \int_{t-\sigma_{i,q}}^{t-\sigma_{i,q-1}} \dot{\tilde{x}}_i(\tau)\,\mathrm{d}\tau\,, \tag{27}$$

where

$$\overline{A}_{i,q}(\Psi_i) = \sum_{k=q}^{m_i} \hat{A}_{i,k}(\Psi_i)\,, \quad q = 0, \ldots, m_i\,. \tag{28}$$

To save space, we will not spell out the argument Ψ_i in $\hat{A}_{i,k}(\Psi_i)$ and $\overline{A}_{i,q}(\Psi_i)$ in the rest of this paper. Then, based on (25) and (27), we provide a sufficient condition for chain consensus in the following theorem.

Theorem 2

Suppose that the head agent 0 moves at a constant speed $v^* \in \mathcal{D}_v$ with $h^* = V^{-1}(v^*) \in \mathcal{D}_h$ (cf. (13) and (18)). Then, the chain can reach consensus if, for each agent i subject to dynamics (2) and (6), there exist positive definite matrices $P_i, Q_{i,1}, \ldots, Q_{i,m_i}, R_{i,2}, \ldots, R_{i,m_i}, W_{i,1}, \ldots W_{i,m_i}$ such that

DOI: 10.1002/rnc

$$\Xi_{i,1} = \begin{bmatrix} Z_i & Y_{i,0,1} & \cdots & Y_{i,0,m_i} & -P_i\overline{A}_{i,1} \\ Y_{i,1,0} & Y_{i,1,1} - Q_{i,1}/\sigma_{i,1} & \cdots & Y_{i,1,m_i} & 0_{2\times 2} \\ \vdots & \vdots & \ddots & \vdots & \vdots \\ Y_{i,m_i,0} & Y_{i,m_i,1} & \cdots & Y_{i,m_i,m_i} - Q_{i,m_i}/\sigma_{i,1} & 0_{2\times 2} \\ -\overline{A}_{i,1}^{\mathrm{T}} P_i & 0_{2\times 2} & \cdots & 0_{2\times 2} & -W_{i,1} \end{bmatrix}, \qquad (29)$$

$$\Xi_{i,q} = \begin{bmatrix} -R_{i,q} & -P_i\overline{A}_{i,q} \\ -\overline{A}_{i,q}^{\mathrm{T}} P_i & -W_{i,q} \end{bmatrix}$$

are negative definite over the domain $\mathcal{D}_h^{i-p_i}$ for $q = 2, \ldots, m_i$, where $0_{2\times 2}$ denotes the two-dimensional zero matrix and

$$\begin{aligned} Y_{i,j,k} &= \frac{1}{\sigma_{i,1}} \left(\sum_{q=1}^{m_i} (\sigma_{i,q} - \sigma_{i,q-1}) \hat{A}_{i,j}^{\mathrm{T}} W_{i,q} \hat{A}_{i,k} \right), \quad j,k = 0, \ldots, m_i, \\ Z_i &= \frac{1}{\sigma_{i,1}} \left(P_i \overline{A}_{i,0} + \overline{A}_{i,0}^{\mathrm{T}} P_i + \sum_{q=1}^{m_i} Q_{i,q} + \sum_{\ell=2}^{m_i} (\sigma_{i,\ell} - \sigma_{i,\ell-1}) R_{i,\ell} + \sigma_{i,1} Y_{i,0,0} \right). \end{aligned} \qquad (30)$$

Note that $\Xi_{i,k}$ in (29) depends on Ψ_i for $k = 1, \ldots, m_i$ (cf. (25) and (28)), while the domain $\mathcal{D}_h^{i-p_i}$ contains all possible values of Ψ_i. The proof of Theorem 2 is given in Appendix B. When applying this theorem, we begin by discretizing the domain $\mathcal{D}_h^{i-p_i}$ and then solve the corresponding linear matrix inequalities (LMIs) numerically for $P_i, Q_{i,1}, \ldots, Q_{i,m_i}, R_{i,2}, \ldots, R_{i,m_i}, W_{i,1}, \ldots, W_{i,m_i}$ by using LMI numerical solvers. Note that the obtained solutions must ensure that the LMIs hold for all values in the domain $\mathcal{D}_h^{i-p_i}$. We remark that there may exist multiple solutions, but we stop the calculation when a solution is found.

Theorem 2 ensures that agent i approaches the consensus equilibrium if its distance and velocity always stay inside the operating domain (18), that is, $z_i(t) \triangleq [h_{i,i-1}(t), v_i(t)]^{\mathrm{T}} \in \mathcal{D}_h \times \mathcal{D}_v$ for all $t \geqslant 0$. Thus, it is also important to find an invariant region inside the operating domain. Here, we name this region as the *feasible region* and define it as follows.

Definition 4
Given a time-delayed system $\dot{z}(t) = f(z(t), z(t-\sigma_1), \ldots, z(t-\sigma_m))$, where $z(t) \in \mathbb{R}^n$ is the state, while $\sigma_1, \ldots, \sigma_m$ denote time delays with σ_m being the maximum time delay. Let $\mathcal{D} \subset \mathbb{R}^n$ be the operating domain. The feasible region $\mathcal{R}_{\mathrm{F}} \subseteq \mathcal{D}$ is defined such that, if $z(\theta) \in \mathcal{R}_{\mathrm{F}}$ for $\forall \theta \in [-\sigma_m, 0]$, then $z(t) \in \mathcal{D}$ for $\forall t \geqslant 0$ and $\lim_{t\to\infty} z(t) = z^*$, where z^* denotes the equilibrium.

Compared with the *region of attraction*

$$\mathcal{R}_{\mathrm{A}} = \left\{ z(\theta) \in C\left([-\sigma_m, 0], \mathbb{R}^n\right) : z\left(t; z(\theta)\right) \text{ is defined for } \forall t \geqslant 0 \text{ and } \lim_{t\to\infty} z\left(t; z(\theta)\right) = z^* \right\} \qquad (31)$$

defined for time delay systems [29], the feasible region is more applicable in our problem due to the following two reasons:

- Feasible region is defined in the finite-dimensional space $\mathbb{R}^n$, while region of attraction is defined in infinite-dimensional space $C\left([-\sigma_m, 0], \mathbb{R}^n\right)$.
- Feasible region takes into account the constraint of the operating domain, while region of attraction does not.

How to calculate the feasible region analytically is a challenging problem and left for future research. Assuming constant initial velocity, we can approximate the feasible region numerically, as will be demonstrated in Section 5.

DOI: 10.1002/rnc

4. DISTURBANCE ATTENUATION

In a network, disturbances arising from an agent affect the behaviors of other agents, which may eventually jeopardize the network consensus. For temporary disturbances, the network consensus may be recovered after transients. Thus, here, we consider persistent disturbances and investigate their impact on the network performance. Input–output disturbance attenuation (15) in $\mathcal{L}_2$ norm can be guaranteed by applying the Hamilton–Jacobi inequality [30]. However, to apply this method to nonlinear time delay systems, one needs to construct a Lyapunov functional for the whole network, which is challenging especially when the network contains a large number of agents. Moreover, the result of the Hamilton–Jacobi inequality is typically quite conservative and may not lead to a solution for large networks. Furthermore, the Hamilton–Jacobi inequality may not guarantee network performance in other $\mathcal{L}_p$ norms such as the $\mathcal{L}_\infty$ norm, which is used to evaluate the largest deviation from the consensus equilibrium. In this section, for input–output disturbance attenuation (15) and eventual disturbance attenuation (16), we seek for simple conditions that can be used in general norms and also remain scalable for large networks.

4.1. Input–output disturbance attenuation

Here, we evaluate the disturbance attenuation by investigating the steady-state response. Because general disturbance signals may not lead to steady-state response, we consider periodic disturbances imposed on the head agent. We begin by providing a sufficient condition that ensures that a periodic input to the nonlinear time-delayed chain ((2) and (6)) leads to periodic steady states with the same period, as stated in the following theorem.

Theorem 3
Consider the multi-agent chain ((2) and (6)) and assume that the disturbance arising from head agent 0 is T-periodic. If Theorem 2 holds, then the steady-state motion of agents $k = 1, \dots, n$ is unique and T-periodic, that is,

$$\tilde{x}_k^{(\mathrm{s})}(t+T) = \tilde{x}_k^{(\mathrm{s})}(t)\,, \quad k = 1, \dots, n\,, \tag{32}$$

where the superscript (s) denotes the steady state.

The proof of Theorem 3 is given in Appendix C. We remark that, for general nonlinear time-delayed chains, periodic disturbances from the head agent do not necessarily lead to periodic motion of the following agents. By applying the controller (6) to the multi-agent chain (2), Theorem 3 can ensure a periodic steady state of the whole chain when a periodic disturbance is imposed on the head agent. This property allows one to investigate the disturbance attenuation by evaluating the frequency response. Thus, in order to investigate the input–output disturbance attenuation (15), we consider sinusoidal disturbances and study the frequency response at the nonlinear level. In particular, for the head agent 0, we assume

$$\tilde{x}_0(t) = \begin{bmatrix} \tilde{s}_0(t) \\ \tilde{v}_0(t) \end{bmatrix} = \begin{bmatrix} v_{\mathrm{amp}} \sin(\omega t)/\omega \\ v_{\mathrm{amp}} \cos(\omega t) \end{bmatrix}, \tag{33}$$

where $v_{\mathrm{amp}} > 0$ and $\omega > 0$ denote the amplitude and the frequency of the disturbance, respectively. Because $\tilde{x}_0(t)$ is periodic with period $T = 2\pi/\omega$, Theorem 3 ensures that the steady states of all following agents are unique and T-periodic. However, due to the nonlinear dynamics, the steady states are not sinusoidal but may be expressed by Fourier series.

To evaluate the frequency response, we define the amplification ratio function

$$\Phi_{n,0}(\omega, v_{\mathrm{amp}}) \triangleq \|\tilde{v}_n^{(\mathrm{s})}\|_{\mathcal{L}_p} / \|\tilde{v}_0\|_{\mathcal{L}_p}\,, \tag{34}$$

which describes how the velocity disturbance arising from the head agent 0 is amplified or attenuated when reaching the tail agent n in steady state. Different norms can be used to characterize the magnitude of signals. Here, we use the $\mathcal{L}_\infty$ norm defined by $\|\tilde{v}\|_{\mathcal{L}_\infty} = \sup_{t>0} |\tilde{v}(t)|$, which accounts

DOI: 10.1002/rnc

for the largest perturbations from the equilibrium. Note that the amplification ratio of nonlinear networks (34) depends on both the input frequency and the input amplitude. This is different from the amplification ratio of linear systems, which is determined only by the input frequency. Then, we present a condition for input–output disturbance attenuation in presence of sinusoidal disturbances, as stated in the following theorem.

Theorem 4
Suppose that Theorem 2 holds and the disturbance imposed on the head agent 0 is sinusoidal given by (33). Then, the input–output disturbance attenuation (15) can be achieved if and only if

$$\sup_{\omega>0} \Phi_{n,0}(\omega, v_{\text{amp}}) < 1\,. \tag{35}$$

The proof can be given by combining Theorem 3 with definitions (15) and (34). To apply Theorem 4, an expression of the steady state of the tail agent n is needed, which may not be obtained in the closed form for general nonlinearities. Here, we approximate the steady-state response by applying Taylor expansion. To improve readability, the details are given in Appendix D. Compared with the harmonic balance approach [31], our results provide analytical approximation of the steady states, which simplifies the analysis and remains scalable for large complex networks. Note that Theorem 4 provides guidelines for choosing control gains but may not guarantee input–output disturbance attenuation for other types of periodic disturbances.

4.2. Eventual disturbance attenuation

Here, we study the eventual disturbance attenuation (16) for the multi-agent chain ((2) and (6)), and we derive a condition that only requires the analysis of the corresponding linearized model.

Linearizing the model ((2) and (6)) about the consensus equilibrium (11) yields

$$\dot{\tilde{x}}_i(t) = A_{i,0}\,\tilde{x}_i(t) + \sum_{j=p_i}^{i-1} A_{i,j}(h^*)\,\tilde{x}_i(t-\xi_{i,j}) + \sum_{j=p_i}^{i-1} B_{i,j}(h^*)\,\tilde{x}_j(t-\xi_{i,j}) \tag{36}$$

(cf. (20)), where the matrices $A_{i,0}$, $A_{i,j}(h^*)$ and $B_{i,j}(h^*)$ are given in (21). Note that these matrices depend on the equilibrium distance h^* that varies with the equilibrium speed v^* (cf. (13)).

Considering the output $\tilde{v}_j(t) = [0 \quad 1]\tilde{x}_j(t)$ for $j = 0, 1, \ldots$ while transforming (36) to the Laplace domain with zero initial condition, we obtain

$$\tilde{V}_i(s) = \sum_{j=p_i}^{i-1} T_{i,j}(s, h^*)\tilde{V}_j(s)\,, \tag{37}$$

where $s \in \mathbb{C}$, $\tilde{V}_i(s)$ denotes the Laplace transform of $\tilde{v}_i(t)$. The link transfer function

$$\begin{aligned} T_{i,j}(s,h^*) &= \mathrm{e}^{-s\xi_{i,j}} C \left(sI_2 - A_{i,0} - \sum_{q=p_i}^{i-1} \mathrm{e}^{-s\xi_{i,q}} A_{i,q}(h^*) \right)^{-1} B_{i,j}(h^*) E(s) \\ &= \frac{\left(\beta_{i,j}\, s + \varphi^*_{i,j}\right) \mathrm{e}^{-s\xi_{i,j}}}{s^2 + \sum_{q=p_i}^{i-1} \left(\kappa_{i,q}\, s + \varphi^*_{i,q}\right) \mathrm{e}^{-s\xi_{i,q}}} \end{aligned} \tag{38}$$

describes how the motion of vehicle j affects the motion of vehicle i, where $C = [0 \quad 1]$, I_2 denotes the two-dimensional identity matrix and

$$E(s) = [s^{-1} \quad 1]^{\mathrm{T}} \tag{39}$$

links the state and the output of agents such that $\tilde{X}_j(s) = E(s)\tilde{V}_j(s)$. The constants $\varphi^*_{i,j} = \varphi_{i,j}(h^*)$ and $\kappa_{i,j}$ are defined in (22).

DOI: 10.1002/rnc

Using link transfer functions (38), one can obtain the head-to-tail transfer function $G_{n,0}(s,h^*)$ that describes the dynamic relationship between the head agent 0 and the tail agent n:

$$\tilde{V}_n(s) = G_{n,0}(s,h^*)\tilde{V}_0(s)\,. \tag{40}$$

To systematically calculate the head-to-tail transfer function for complex networks in an efficient way, one can apply the approach presented in [3] that contains the following three steps:

(1) Construct the coupling matrix $T(s,h^*) = [T_{i,j}(s,h^*)] \in \mathbb{C}^{(n+1)\times(n+1)}$ for $i,j = 0,1,\ldots,n$, where $T_{i,j}(s,h^*)$ is given in (38).
(2) Modify the coupling matrix as

$$\widehat{T}(s,h^*) = R\left(T(s,h^*) + I_{n+1}\right)R^{\mathrm{T}}\,, \tag{41}$$

where $R = [0_{n\times 1} \quad I_n] \in \mathbb{R}^{n\times(n+1)}$ and I_n denotes the n-dimensional identity matrix while $0_{n\times 1}$ is an n-by-1 zero vector. Indeed, $\widehat{T}(s,h^*)$ can be obtained by deleting the first row and the last column of the matrix $T(s,h^*) + I_{n+1}$.
(3) Calculate the head-to-tail transfer function by using the 'determinant-like' formula

$$G_{n,0}(s,h^*) = \sum_{\mu_i \in S_n} \prod_{i=1}^{n} \widehat{T}_{i,\mu_i}(s,h^*)\,, \tag{42}$$

where the sum is computed over all permutations of the set $S_n = \{1,2,\ldots,n\}$. Note that formula (42) is similar to the determinant of $\widehat{T}(s)$ but does not include the sign changes.

Readers interested in this approach may refer to [3] for more details and examples. Note that the explicit expression of link transfer functions (38) and the formula (42) provide an efficient way to calculate the head-to-tail transfer function for large networks with complex topologies. Now, we provide a sufficient condition for the eventual disturbance attenuation (16) in the following theorem.

Theorem 5
For the multi-agent chain ((2) and (6)), the disturbance arising from the head agent 0 can be attenuated in the sense of (16) if all the following conditions hold:

- Theorem 2 holds.
- The range policy function $V(h)$ in (6) satisfies

$$\left|\frac{\mathrm{d}^{k+1}V(h)}{\mathrm{d}h^{k+1}}\right| < \left|\frac{\mathrm{d}^{k}V(h)}{\mathrm{d}h^{k}}\right| < 1 \qquad \text{and} \qquad \lim_{n\to\infty}\left|\frac{\mathrm{d}^{n}V(h)}{\mathrm{d}h^{n}}\right| = 0\,, \tag{43}$$

for all $k > 1$ and for all $h_{\mathrm{st}} < h < h_{\mathrm{go}}$.
- The magnitude of the head-to-tail transfer function (40) is always smaller than 1, that is,

$$\sup_{\omega>0,\, h^*\in\mathcal{D}_h} |G_{n,0}(\mathrm{j}\omega,h^*)| < 1, \tag{44}$$

where $\mathrm{j}^2 = -1$.

The proof is given in Appendix E. We remark that in practice, empirical traffic data show that the range policies of human drivers may satisfy (43); see [14]. Theorem 5 reduces the analysis complexity in two aspects. On one hand, it allows one to analyze disturbance attenuation in nonlinear chains by only studying the linearized model. On the other hand, it allows one to ensure the performance of cascading chains by only analyzing the dynamics of a single block. Note that in Theorem 5, one must ensure that condition (44) holds for all possible values of h^* in the domain $\mathcal{D}_h$ defined in (18). This is different from the analysis of the linearized dynamics, which only needs to satisfy (44) for certain value of $h^* \in \mathcal{D}_h$.

DOI: 10.1002/rnc

5. CASE STUDY AND SIMULATIONS

In this section, we apply the theorems presented in Sections 3 and 4 to a connected vehicle network shown in Figure 2. Neglecting the effects of air drag and rolling resistance in the physics-based vehicle model [32, 33] leads to the simplified longitudinal model in the form (2). We assume that all vehicles are driven by human drivers with reaction time $\xi_{k,k-1} = 0.5$ [s] and fixed control gains $\alpha_{k,k-1} = 0.3$ [1/s] and $\beta_{k,k-1} = 0.5$ [1/s] for $k = 1, 2, \ldots$. Moreover, we assume that every $(2k-1)$-st vehicle is non-autonomous, while every $2k$-th vehicle is semi-autonomous. We consider communication delay to be $\xi_{k,j} = 0.2$ [s] for $j < k-1$, $k = 1, 2, \ldots$. We use

$$F(h) = \frac{v_{\max}}{2}\left(1 - \cos\left(\pi \frac{h - h_{\rm st}}{h_{\rm go} - h_{\rm st}}\right)\right) \tag{45}$$

in the range policy (5) such that the function $V(h)$ is continuously differentiable at $h = h_{\rm st}$ and $h = h_{\rm go}$, which can improve the ride comfort. According to traffic data given in [14], we set $h_{\rm st} = 5$ [m], $h_{\rm go} = 35$ [m] and $v_{\max} = 30$ [m/s]. Moreover, we assume the desired operating domain

$$\mathcal{D}_h = \{h : 15 \leqslant h \leqslant 25 \text{ [m]}\}, \quad \mathcal{D}_v = \{v : 0 \leqslant v \leqslant 30 \text{ [m/s]}\}. \tag{46}$$

For such vehicle network, a study based on linearized dynamics has been presented in [3]. In the following part, we compare those results with the results obtained by the nonlinear analysis presented in this paper.

In particular, we consider the vehicle network in Figure 2 with 41 vehicles and design control gains $\alpha_{k,k-m}, \beta_{k,k-m}$ $(m = 2, 3)$ by applying Theorems 2, 4 and 5, in order to exploit the information received via wireless communication. Fixing $\alpha_{k,k-2} = 0$ [1/s] and $\beta_{k,k-2} = 1$ [1/s], we derive conditions for choosing control gains $\alpha_{k,k-3}, \beta_{k,k-3}$ and display the results using stability diagrams as shown in Figure 3(a) and (b). Here, the control gains inside the gray-shaded domain can ensure chain consensus (12). Besides consensus, the control gains from the '\'-shaded and the '/'-shaded areas can also achieve input–output disturbance attenuation (15) and eventual disturbance attenuation (16), respectively. The solid red curve (enclosing the gray-shaded domain), the solid black curve and the solid blue curve mark the boundaries resulting from Theorems 2, 4 and 5, respectively. The dashed red and the dashed blue curves are derived by using the linearized model for consensus and disturbance attenuation, respectively [3].

To evaluate the effects of the long-range communication on the network performance, we first consider the network without communication as a benchmark, which corresponds to $\alpha_{k,k-2} = \beta_{k,k-2} = \alpha_{k,k-3} = \beta_{k,k-3} = 0$ for all k (see Figure 2 without red links). Then, we exploit the communication and choose two sets of control gains corresponding to the points marked by A and B in Figure 3(b). To test the robustness, we consider an extreme case where the consensus equilibrium is at the boundary of the operating domain (46) that is enclosed by the red dashed-dotted curve in Figure 3(c) and (d). In particular, we consider the equilibrium distance $h^* = 25$ [m] that leads to the equilibrium speed $v^* = 22.5$ [m/s] (cf. (5), (13) and (45)).The equilibrium is highlighted by the black star in Figure 3(c) and (d). Assuming constant initial velocities, that is, $v_i(\theta) \equiv v_{i,0}$ and $s_i(\theta) = s_{i,0} + v_{i,0}(\theta + 0.5)$ for $\forall \theta \in [-0.5, 0]$, we obtain the feasible regions for cases A and B numerically, as displayed in Figure 3(c) and (d), respectively. To simulate consensus, we let vehicle 0 move at a constant speed $v_0(t) \equiv v^* = 22.5$ [m/s] with initial position $s_{0,0} = 0$ [m]. The initial conditions for following agents are given by $v_{i,0} = 25$ [m/s] and $s_{i,0} = -21i$ [m] for $i = 1, \ldots, 40$. The corresponding simulation results for the benchmark and for cases A and B are shown in Figure 4, where the top row displays the distance between vehicles 39 and 40, while the bottom row shows the speed of vehicle 40. Although the benchmark case can eventually achieve consensus, the settling time is long, and there exist undesired transient oscillations that push states outside the operating domain (46) (Figure 4(a) and (d)). For case A (Figure 4(b) and (d)), such undesired transients are avoided, while there is a small overshoot around $t = 40$ [s] where the distance is outside the operating domain (see the zoomed-in panel in Figure 4(b)). The gains corresponding to point B are chosen to ensure both input–output and eventual disturbance attenuation. Now, consensus is achieved without overshoot (Figure 4(c) and (f)). Comparison between cases A

DOI: 10.1002/rnc

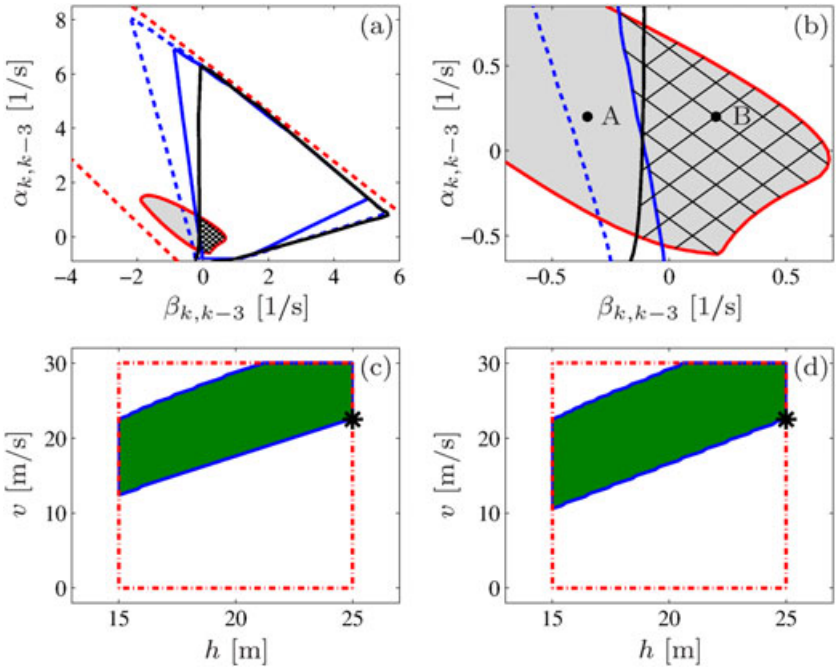

Figure 3. (a) Stability diagram in $(\beta_{k,k-3}, \alpha_{k,k-3})$-plane for consensus and disturbance attenuation. Gray-shaded, '\'-shaded and '/'-shaded highlight the domains for consensus, input–output disturbance attenuation and eventual disturbance attenuation, respectively. Solid red, solid black and solid blue curves are obtained by using Theorems 2, 4 and 5, respectively. The dashed red and the dashed blue curves enclose domains for consensus and disturbance attenuation that are obtained using linearized models [3]. (b) A zoomed-in view of panel (a). (c) and (d) Feasible regions (shaded) for cases A and B, respectively. The red dashed-dotted lines bound the operating domain $\mathcal{D}_h \times \mathcal{D}_v$ and the black star denotes the equilibrium.

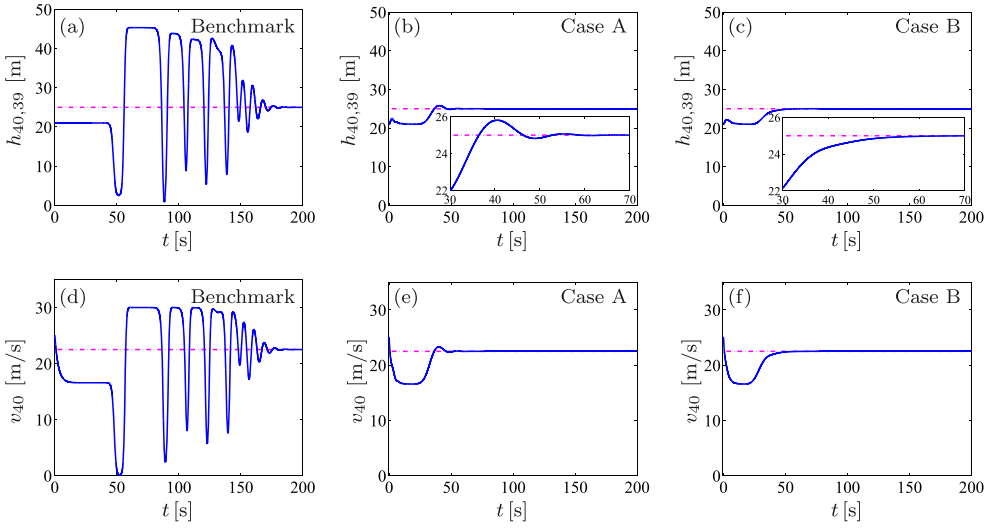

Figure 4. Simulation results for consensus. The top row shows the distance between vehicles 39 and 40, while the bottom row shows the velocity of vehicle 40, respectively. Dashed-dotted lines indicate the consensus equilibrium.

and B implies that, although our results for disturbance attenuation are obtained by analyzing the steady-state response, they may also improve the transient behavior.

To test disturbance attenuation, we consider a sinusoidal velocity disturbance $v_0(t) = v^* + v_{\text{amp}} \cos(\omega t)$ for vehicle 0, where $v_{\text{amp}} = 6$ [m/s] and $\omega = 0.18$ [rad/s]. Using the same initial

DOI: 10.1002/rnc

conditions as used for consensus, we conduct simulations for the benchmark and for cases A and B. The results are displayed in Figure 5, where the top row demonstrates how the disturbance evolves when propagating along the network, while the bottom row shows the velocities of vehicles 0 and 40. In the benchmark where the communication is not exploited, the disturbance arising from vehicle 0 is amplified when propagating to following vehicles and leads to stop-and-go motion for vehicle 40 (Figure 5(a) and (d)). The saturations at $v = 0$ [m/s] and $v = 30$ [m/s] are caused by the saturation of the function (5) with $v_{\max} = 30$ [m/s]. Figure 3(b) shows that point A is inside the region for disturbance attenuation obtained by linear analysis but outside the corresponding regions obtained by nonlinear analysis. Simulation results in Figure 5(b) and (e) demonstrate that the disturbance is indeed amplified as it propagates along the chain. This implies that the results obtained from linearized dynamics may be not valid when perturbations are large. The control gains at point B are chosen inside the region for input–output and eventual disturbance attenuation. Simulations in Figure 5(c) and (f) show that the disturbance is attenuated along the chain although not uniformly because it is amplified by non-autonomous (human-driven) vehicles.

For case A, we also investigate the frequency response by comparing the result obtained by linear analysis [3] with that obtained by nonlinear approximation derived in this paper. Figure 6(a) displays the amplification curves obtained via linear approximation (green), nonlinear approximation (red) and numerical simulation (blue). It shows that the nonlinear analysis is more accurate

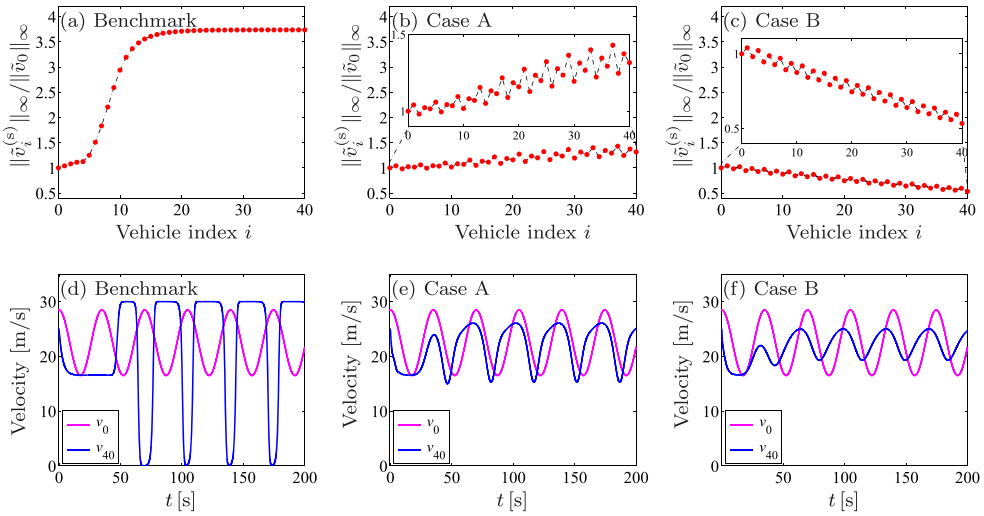

Figure 5. Simulation results for disturbance attenuation. In the top row, the red points show the amplification ratios between the perturbation of each following vehicle and that of the leading vehicle in terms of $\mathcal{L}_\infty$ norm, while the bottom row displays the velocities of vehicles 0 and 40, respectively.

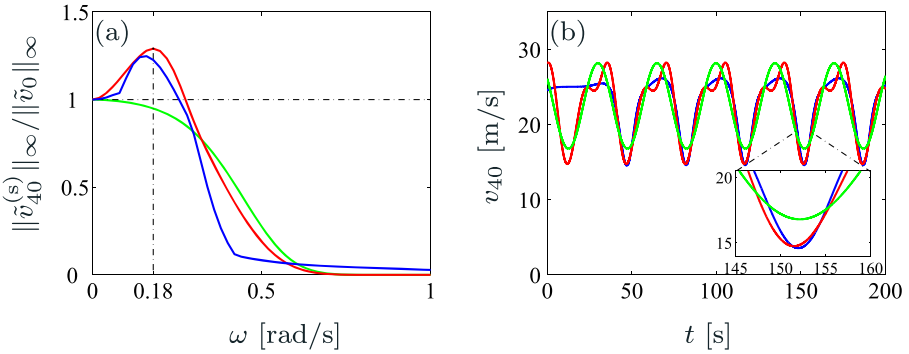

Figure 6. Comparison of the linear approximation (green) and the nonlinear approximation (red) with the numerical simulation (blue). (a) Amplification ratio curves and (b) velocity of the tail vehicle 40.

DOI: 10.1002/rnc

than the linear analysis. In particular, the nonlinear analysis reveals the disturbance amplification, which cannot be achieved by the linear analysis. Choosing $\omega = 0.18$, [rad/s], we also compare the approximation and the numerical simulation as shown in Figure 6(b), which shows that the nonlinear approximation captures the largest perturbation better and hence characterize the input–output disturbance attenuation (see the zoomed-in inlet in Figure 6(b)).

6. CONCLUSION

In this paper, we investigated consensus and disturbance attenuation in multi-agent chains that included NAAs, SAAs and AAs. Resembling the predetermined dynamics of NAAs, we presented a nonlinear control framework that included information delays and allowed a large variety of connectivity topologies. This framework can guarantee the existence of a unique consensus equilibrium that is independent of the network size, connectivity topologies, control gains and information delays. For consensus and disturbance attenuation, we presented conditions that remain scalable for large complex networks. Numerical simulation was used to validate the analytical results and demonstrate the necessity for ensuring disturbance attenuation in consensus networks.

Although disturbance attenuation has positive impacts for avoiding collisions, it does not necessarily guarantee collision avoidance in practice. In the future, we will extend the current work by incorporating explicit safety considerations into design. Moreover, the agents in this paper are described by the point mass model. Extending the results to physics-based models is also left for future research.

APPENDIX A: PROOF OF THEOREM 1

Considering (2), (6) and (7), we have

$$\begin{aligned}\dot{h}_{i,i-1}(t) &= v_{i-1}(t) - v_i(t)\,,\\ \dot{v}_i(t) &= \sum_{j=p_i}^{i-1}\left[\alpha_{i,j}\left(V\left(h_{i,j}(t-\xi_{i,j})\right) - v_i(t-\xi_{i,j})\right) + \beta_{i,j}\left(v_j(t-\xi_{i,j}) - v_i(t-\xi_{i,j})\right)\right].\end{aligned} \tag{47}$$

To determine the equilibrium of agent i, we assume that all agents ahead have reached the consensus equilibrium, that is, $h^*_{j,j-1}(t) \equiv h^*$ and $v^*_j(t) \equiv v^* = V(h^*)$ for $j = 1, \ldots, i-1$. Then, at equilibrium, agent i satisfies

$$\begin{aligned}0 &= v^* - v^*_i(t)\,,\\ 0 &= \sum_{j=p_i}^{i-1}\left[\alpha_{i,j}\left(V\left(h^*_{i,j}(t-\xi_{i,j})\right) - v^*_i(t-\xi_{i,j})\right) + \beta_{i,j}\left(v^* - v^*_i(t-\xi_{i,j})\right)\right].\end{aligned} \tag{48}$$

The first equation in (48) yields $v^*_i(t) \equiv v^*$. Substituting this into the second equation in (48) yields

$$0 = \sum_{j=p_i}^{i-1}\alpha_{i,j}\left(V\left(h^*_{i,j}(t-\xi_{i,j})\right) - v^*\right). \tag{49}$$

Then, we will prove

$$h^*_{i,i-1}(t) \equiv h^* = V^{-1}(v^*) \tag{50}$$

for all $i = 1, \ldots, n$ by induction. When $i = 1$, (49) becomes

$$0 = \alpha_{1,0}\left(V\left(h^*_{1,0}(t-\xi_{1,0})\right) - v^*\right). \tag{51}$$

According to (5), $0 < v^* < v_{\max}$ implies that $h_{\mathrm{st}} < h^*_{1,0}(t) < h_{\mathrm{go}}$. In this region, $V(h)$ is continuous and strictly monotonically increasing so that the inverse of $V(h)$ exists. As $\alpha_{1,0} > 0$, Eq. (51) has a unique solution

DOI: 10.1002/rnc

$$h^*_{1,0}(t) \equiv V^{-1}(v^*) = h^* \,. \tag{52}$$

For induction, we assume

$$h^*_{i,i-1}(t) \equiv V^{-1}(v^*) = h^* \,, \tag{53}$$

for $i = 1, \ldots, k$, where $k \geqslant 1$. Then, one needs to prove that

$$h^*_{k+1,k}(t) \equiv V^{-1}(v^*) = h^* \tag{54}$$

is also the unique solution of (49).

Based on (53), one trivial solution of (49) for $i = k + 1$ is given by (54). Then, we show that this solution is unique. Equation (49) for $i = k + 1$ can be rewritten as

$$\sum_{j=p_{k+1}}^{k} \alpha_{k+1,j} V\left(h^*_{k+1,j}(t - \xi_{k+1,j})\right) = \sum_{j=p_{k+1}}^{k} \alpha_{k+1,j} v^* \,. \tag{55}$$

Because $\alpha_{k+1,j} \geqslant 0$ for $j = p_{k+1}, \ldots, k-1$, $\alpha_{k+1,k} > 0$ and $h^*_{k+1,j}(t)$ only depends on $h^*_{k+1,k}(t)$, the left-hand side of (55) is a strictly monotonically increasing function of $h^*_{k+1,k}(t)$. As the right-hand side of (55) is a constant, the solution is unique if there exists one. Therefore, (54) is the unique equilibrium of agent $k + 1$. This completes the proof.

APPENDIX B: PROOF OF THEOREM 2

The asymptotic stability of the consensus equilibrium is proved by using the Lyapunov–Krasovskii theorem. Here, we use the positive definite functional

$$L = \tilde{x}_i^{\mathrm{T}}(t)\, P_i\, \tilde{x}_i(t) + \sum_{j=1}^{m_i} \int_{t-\sigma_{i,j}}^{t} \tilde{x}_i^{\mathrm{T}}(\tau)\, Q_{i,j}\, \tilde{x}_i(\tau)\, \mathrm{d}\tau + \sum_{j=1}^{m_i} \int_{-\sigma_{i,j}}^{-\sigma_{i,j-1}} \int_{t+\theta}^{t} \dot{\tilde{x}}_i^{\mathrm{T}}(\tau)\, W_{i,j}\, \dot{\tilde{x}}_i(\tau)\, \mathrm{d}\tau \mathrm{d}\theta \,, \tag{56}$$

where matrices P_i, $Q_{i,j}$ and $W_{i,j}$ are all positive definite for $j = 1, \ldots, m_i$. Substituting (25) and (27) into the time derivative of (56) and adding

$$0 = \sum_{\ell=2}^{m_i} (\sigma_{i,q} - \sigma_{i,q-1}) \tilde{x}_i^{\mathrm{T}}(t)\, R_{i,q}\, \tilde{x}_i(t) - \sum_{\ell=2}^{m_i} \int_{t-\sigma_{i,q}}^{t-\sigma_{i,q-1}} \tilde{x}_i^{\mathrm{T}}(t)\, R_{i,q}\, \tilde{x}_i(t)\, \mathrm{d}\tau \tag{57}$$

yields

$$\begin{aligned} \dot{L} = \Delta_i(t) &- \sum_{j=1}^{m_i} 2\tilde{x}_i^{\mathrm{T}}(t) P_i \overline{A}_{i,j} \int_{t-\sigma_{i,j}}^{t-\sigma_{i,j-1}} \dot{\tilde{x}}_i(\tau)\, \mathrm{d}\tau - \sum_{j=1}^{m_i} \int_{t-\sigma_{i,j}}^{t-\sigma_{i,j-1}} \dot{\tilde{x}}_i^{\mathrm{T}}(\tau) W_{i,j} \dot{\tilde{x}}(\tau)\, \mathrm{d}\tau \\ &- \sum_{q=2}^{m_i} \int_{t-\sigma_{i,q}}^{t-\sigma_{i,q-1}} \tilde{x}_i^{\mathrm{T}}(t) R_{i,q} \tilde{x}_i(t)\, \mathrm{d}\tau \,, \end{aligned} \tag{58}$$

where

$$\begin{aligned} \Delta_i(t) = {} & \sigma_{i,1} \tilde{x}_i^{\mathrm{T}}(t)(Z_i - Y_{i,0,0}) \tilde{x}_i(t) - \sum_{j=1}^{m_i} \tilde{x}_i^{\mathrm{T}}(t - \sigma_{i,j}) Q_{i,j} \tilde{x}_i(t - \sigma_{i,j}) \\ & + \left(\sum_{k=0}^{m_i} \hat{A}_{i,k} \tilde{x}_i(t - \sigma_{i,k}) \right)^{\mathrm{T}} \left(\sum_{q=1}^{m_i} (\sigma_{i,q} - \sigma_{i,q-1}) W_{i,q} \right) \left(\sum_{k=0}^{m_i} \hat{A}_{i,k} \tilde{x}_i(t - \sigma_{i,k}) \right) \,, \end{aligned} \tag{59}$$

and $Y_{i,0,0}$ and Z_i are given in (30). Then, substituting the identity

DOI: 10.1002/rnc

$$\Delta_i(t) = \frac{1}{\sigma_{i,1}} \int_{t-\sigma_{i,1}}^{t} \Delta_i(t)\, \mathrm{d}\tau \tag{60}$$

into (58) and writing the results in matrix form results in

$$\dot{L} = \int_{t-\sigma_{i,1}}^{t} \tilde{\chi}_i^{\mathrm{T}}(t,\tau)\Xi_{i,1}(\Psi_i)\tilde{\chi}_i(t,\tau)\, \mathrm{d}\tau + \sum_{q=2}^{m_i} \int_{t-\sigma_{i,q}}^{t-\sigma_{i,q-1}} \tilde{X}_i^{\mathrm{T}}(t,\tau)\Xi_{i,q}(\Psi_i)\tilde{X}_i(t,\tau)\, \mathrm{d}\tau\,, \tag{61}$$

where $\tilde{\chi}_i^{\mathrm{T}}(t,\tau) = \left[\tilde{x}_i^{\mathrm{T}}(t-\sigma_{i,0}), \ldots, \tilde{x}_i^{\mathrm{T}}\left(t-\sigma_{i,m_i}\right), \dot{\tilde{x}}_i^{\mathrm{T}}(\tau)\right]$ and $\tilde{X}_i^{\mathrm{T}}(t,\tau) = \left[\tilde{x}_i^{\mathrm{T}}(t), \dot{\tilde{x}}_i^{\mathrm{T}}(\tau)\right]$ while $\Xi_{i,1}(\Psi_i)$ and $\Xi_{i,q}(\Psi_i)$ for $q = 2, \ldots, m_i$ are given in (29).

Suppose that the eigenvalues and the corresponding normalized eigenvectors of $\Xi_{i,j}(\Psi_i)$ are given by $\lambda_{j,k}(\Psi_i)$ and $\eta_{j,k}(\Psi_i)$, respectively, for $j = 1, \ldots, m_i$ and $k = 1, \ldots, n_j$, where $n_1 = 2m_i + 4$ and $n_j = 4$ for $j = 2, \ldots, m_i$ (cf. (29)). Because $\Xi_{i,j}(\Psi_i)$ is symmetric, the eigenvectors $\eta_{j,1}(\Psi_i), \ldots, \eta_{j,n_j}(\Psi_i)$ are orthogonal to each other for $\forall \Psi_i \in \mathcal{D}_h^{i-p_i}$ and for $j = 1, \ldots, m_i$. Then, the matrices

$$\begin{aligned} \Lambda_j(\Psi_i) &= \mathrm{diag}\left\{\lambda_{j,1}(\Psi_i), \ldots, \lambda_{j,n_j}(\Psi_i)\right\}, \\ T_j(\Psi_i) &= \left[\eta_{j,1}(\Psi_i), \ldots, \eta_{j,n_j}(\Psi_i)\right] \end{aligned} \tag{62}$$

have the following properties:

$$T_j(\Psi_i)\, T_j^{\mathrm{T}}(\Psi_i) = I\,, \quad \text{and} \quad T_j^{\mathrm{T}}(\Psi_i)\, \Xi_{i,j}(\Psi_i)\, T_j(\Psi_i) = \Lambda_j(\Psi_i)\,, \tag{63}$$

for $j = 1, \ldots, m_i$. Indeed, $\Lambda_j(\Psi_i)$ is negative definite for $\forall \Psi_i \in \mathcal{D}_h^{i-p_i}$ because $\Xi_{i,j}(\Psi_i)$ is negative definite for $\forall \Psi_i \in \mathcal{D}_h^{i-p_i}$.

Let

$$\begin{aligned} \Theta_1(\Psi_i,t,\tau) &= \left[\theta_{1,k}(\Psi_i,t,\tau)\right] = T_1^{\mathrm{T}}(\Psi_i)\, \tilde{\chi}_i(t,\tau)\,, \\ \Theta_j(\Psi_i,t,\tau) &= \left[\theta_{j,k}(\Psi_i,t,\tau)\right] = T_j^{\mathrm{T}}(\Psi_i)\, \tilde{X}_i(t,\tau) \end{aligned} \tag{64}$$

(cf. (61)). Then, it follows that

$$\begin{aligned} \tilde{\chi}_i^{\mathrm{T}}(t,\tau)\, \Xi_{i,1}(\Psi_i)\, \tilde{\chi}_i(t,\tau) &= \Theta_1^{\mathrm{T}}(\Psi_i,t,\tau)\, \Lambda_1(\Psi_i)\, \Theta_1(\Psi_i,t,\tau) = \sum_{k=1}^{n_1} \lambda_{1,k}(\Psi_i)\, \theta_{1,k}^2(\Psi_i,t,\tau)\,, \\ \tilde{X}_i^{\mathrm{T}}(t,\tau)\, \Xi_{i,j}(\Psi_i)\, \tilde{X}_i(t,\tau) &= \Theta_j^{\mathrm{T}}(\Psi_i,t,\tau)\, \Lambda_j(\Psi_i)\, \Theta_j(\Psi_i,t,\tau) = \sum_{k=1}^{n_j} \lambda_{j,k}(\Psi_i)\, \theta_{j,k}^2(\Psi_i,t,\tau) \end{aligned} \tag{65}$$

are negative definite for $\forall \Psi_i \in \mathcal{D}_h^{i-p_i}$ and $j = 2, \ldots, m_i$. Considering this in (61), $\dot{L}$ becomes negative definite because the integration does not change the negative sign. The only solution for $\dot{L} = 0$ is $\Theta_j(\Psi_i,t,\tau) = 0$ for $j = 1, \ldots, m_i$. It follows that $\tilde{\chi}_i(t,\tau) = 0$ and $\tilde{X}_i(t,\tau) = 0$ is the unique solution for $\dot{L} = 0$, implying that $\tilde{x}_i(t) \to 0$ as $t \to \infty$.

APPENDIX C: PROOF OF THEOREM 3

First, we study the steady states of agent i by assuming that states of agents $j = 0, 1, \ldots, i-1$ are T-periodic such that

$$e_j(t) = \begin{bmatrix} e_{j,s}(t) \\ e_{j,v}(t) \end{bmatrix} \triangleq \begin{bmatrix} s_j(t+T) - s_j(t) \\ v_j(t+T) - v_j(t) \end{bmatrix} \equiv 0\,. \tag{66}$$

Substituting $t = t + T$ into the closed-loop system ((2) and (6)), subtracting the result from ((2) and (6)) while considering the definition (66) for $j = i$, we obtain

DOI: 10.1002/rnc

$$\dot{e}_i(t) = \begin{bmatrix} e_{i,v}(t) \\ \sum_{j=p_i}^{i-1} \alpha_{i,j} \left(V\left(h_{i,j}(t+T-\xi_{i,j})\right) - V\left(h_{i,j}(t-\xi_{i,j})\right)\right) - \kappa_{i,j} e_{i,v}(t-\xi_{i,j}) \end{bmatrix}. \quad (67)$$

When $h_{i,j}(t) \in \mathcal{D}_h$, according to the mean value theorem, there exists $\mu_{i,j} \in \mathcal{D}_h$ such that

$$V\left(h_{i,j}(t+T)\right) - V\left(h_{i,j}(t)\right) = -\frac{V'(\mu_{i,j})}{i-j} e_{i,s}(t)\,. \quad (68)$$

Substituting (68) into (67) yields

$$\dot{e}_i(t) = A_0\, e_i(t) + \sum_{j=p_i}^{i-1} A_{i,j}(\mu_{i,j})\, e_i(t-\xi_{i,j})\,. \quad (69)$$

Similar to (23)–(25), we collect terms according to distinct delays $\sigma_{i,k}$ for $k = 0, \ldots, m_i$ and obtain

$$\dot{e}_i(t) = \sum_{k=0}^{m_i} \hat{A}_{i,k}(U_i)\, e_i(t-\sigma_{i,k})\,, \quad (70)$$

where $U_i = [\mu_{i,p_i}, \ldots, \mu_{i,i-1}]$. Note that (70) is equivalent to (25) because $\hat{A}_{i,k}(U_i)$ and $\hat{A}_{i,k}(\Psi_i)$ have the same bound for all $U_i, \Psi_i \in \mathcal{D}_h^{i-p_i}$. Therefore, $e_i(t) = 0$ is asymptotically stable for (70) if $\tilde{x}_i(t) = 0$ if asymptotically stable for (25), which implies that $\lim_{t\to\infty} e_i(t) = 0$ if Theorem 2 holds and $e_j(t) = 0$ for $j = p_i, \ldots, i-1$. Because agent 1 only responds to agent 0, when the disturbance imposed on agent 0 is T-periodic (i.e. $e_0(t) \equiv 0$), it follows that $\lim_{t\to\infty} e_1(t) = 0$. Repeating this process to agents $j = 2, \ldots, n$, one can show that the steady states of all agents in the network are T-periodic.

Then, we prove the uniqueness of the periodic steady states by contradiction. We assume that the steady states of agents $j = 0, 1, \ldots, i-1$ are unique but agent i has two distinct steady-state trajectories corresponding to different initial conditions. We denote these two steady-state trajectories by $s_i^{(1)}(t)$, $v_i^{(1)}(t)$ and $s_i^{(2)}(t)$, $v_i^{(2)}(t)$, of which the dynamics is governed by

$$\begin{aligned} \dot{s}_i^{(k)}(t) &= v_i^{(k)}(t)\,, \\ \dot{v}_i^{(k)}(t) &= \sum_{j=p_i}^{i-1} \alpha_{i,j} \left(V\left(h_{i,j}^{(k)}(t-\xi_{i,j})\right) - v_i^{(k)}(t-\xi_{i,j})\right) + \beta_{i,j}\left(v_j(t-\xi_{i,j}) - v_i^{(k)}(t-\xi_{i,j})\right), \end{aligned} \quad (71)$$

for $k = 1, 2$, where $h_{i,j}^{(k)}(t) = \left(s_j(t) - s_i^{(k)}(t) - \sum_{q=j}^{i-1} l_q\right)/(i-j)$ (cf. (2)–(7)). Subtracting (71) with $k = 1$ from (71) with $k = 2$ yields

$$\begin{aligned} \dot{\zeta}_i(t) &= v_i(t)\,, \\ \dot{v}_i(t) &= \sum_{j=p_i}^{i-1} \alpha_{i,j} \left(V\left(h_{i,j}^{(1)}(t-\xi_{i,j})\right) - V\left(h_{i,j}^{(2)}(t-\xi_{i,j})\right)\right) - \kappa_{i,j} v_i(t-\xi_{i,j})\,, \end{aligned} \quad (72)$$

where $\zeta_i(t) = s_i^{(1)}(t) - s_i^{(2)}(t)$ and $v_i(t) = v_i^{(1)}(t) - v_i^{(2)}(t)$. When $h_{i,j}^{(1)}(t), h_{i,j}^{(2)}(t) \in \mathcal{D}_h$ holds for all $t \geqslant 0$, one can apply the mean value theorem and obtain variables $\vartheta_{i,j} \in \mathcal{D}_h$ such that

$$V\left(h_{i,j}^{(1)}(t)\right) - V\left(h_{i,j}^{(2)}(t)\right) = -\frac{V'(\vartheta_{i,j})}{i-j}\zeta_i(t)\,. \quad (73)$$

Defining $\phi_i(t) = [\zeta_i(t),\ v_i(t)]^{\mathrm{T}}$ and plugging (73) into (72) leads to

$$\dot{\phi}_i(t) = A_{i,0}\,\phi_i(t) + \sum_{j=p_i}^{i-1} A_{i,j}(\vartheta_{i,j})\,\phi_i(t-\xi_{i,j})\,. \quad (74)$$

DOI: 10.1002/rnc

Similar to (23)–(25), we collect terms according to distinct delays $\sigma_{i,k}$ for $k = 0, \ldots, m_i$ and obtain

$$\dot{\phi}_i(t) = \sum_{k=0}^{m_i} \hat{A}_{i,k}(\vartheta_i)\, \phi_i(t - \sigma_{i,k})\,, \tag{75}$$

where $\vartheta_i = [\vartheta_{i,p_i}, \ldots, \vartheta_{i,i-1}]$. This system is equivalent to (25), because $\hat{A}_{i,k}(\vartheta_i)$ and $\hat{A}_{i,k}(\Psi_i)$ have the same bound for all $\vartheta_i, \Psi_i \in \mathcal{D}_h^{i-p_i}$. Therefore, if Theorem 2 holds, we have $\lim_{t\to\infty} \phi_i(t) = 0$, implying that $s_i^{(1)}(t) = s_i^{(2)}(t)$ and $v_i^{(1)}(t) = v_i^{(2)}(t)$ at the steady state, which contradicts our original assumption. Hence, the periodic steady state is unique.

APPENDIX D: APPROXIMATION OF THE STEADY STATE

Applying Taylor expansion to the system ((2) and (6)) about the consensus equilibrium (11) yields

$$\begin{aligned} \dot{\tilde{x}}_i(t) &= A_{i,0}\, \tilde{x}_i(t) + \sum_{j=p_i}^{i-1} \left[A_{i,j}^*\, \tilde{x}_i(t - \xi_{i,j}) + B_{i,j}^*\, \tilde{x}_j(t - \xi_{i,j})\right] + F_i\,, \\ \tilde{y}_i(t) &= C\, \tilde{x}_i(t)\,, \end{aligned} \tag{76}$$

where $A_{i,0}$, $A_{i,j}^* = A_{i,j}(h^*)$, $B_{i,j}^* = B_{i,j}(h^*)$ are given in (21), $C = [0\ 1]$,

$$F_i = \begin{bmatrix} 0 \\ \sum_{j=p_i}^{i-1} \alpha_{i,j} \sum_{m=2}^{M} \epsilon_m \left(\frac{\tilde{s}_j(t-\xi_{i,j}) - \tilde{s}_i(t-\xi_{i,j})}{i-j}\right)^m \end{bmatrix}, \tag{77}$$

and M denotes the order of Taylor expansion, and $\epsilon_m = \frac{1}{m!}\frac{\mathrm{d}^m V(h^*)}{\mathrm{d}h^m}$. Defining $\epsilon = [\epsilon_2, \ldots, \epsilon_M]$, one can express the solution of (76) as $\tilde{x}_i(t, \epsilon)$ and $\tilde{y}_i(t, \epsilon)$. To make the following expressions more compact, we also define a vector $r = [r_2, \ldots, r_M]$ such that

$$\epsilon^r \triangleq \prod_{m=2}^{M} \epsilon_m^{r_m}\,. \tag{78}$$

Moreover, we define $|r| \triangleq \sum_{m=2}^{M} r_m$. Then, we apply Taylor expansion to $\tilde{x}_i(t, \epsilon)$ and $\tilde{y}_i(t, \epsilon)$ about $\epsilon = 0$ up to the order R, which leads to

$$\tilde{x}_i(t, \epsilon) = \sum_{|r|=0}^{R} \epsilon^r\, \tilde{x}_{i,r}(t)\,, \quad \tilde{y}_i(t, \epsilon) = \sum_{|r|=0}^{R} \epsilon^r\, \tilde{y}_{i,r}(t)\,. \tag{79}$$

Substituting (79) into (76) and (77) while matching coefficients of ϵ^r yields

$$\begin{aligned} \dot{\tilde{x}}_{i,r}(t) &= A_{i,0}\tilde{x}_{i,r}(t) + \sum_{j=p_i}^{i-1} \left[A_{i,j}^*\, \tilde{x}_{i,r}(t - \xi_{i,j}) + B_{i,j}^*\, \tilde{x}_{j,r}(t - \xi_{i,j})\right] + f_{i,r}\left(X_{i,\hat{r}}(t)\right)\,, \\ \tilde{y}_{i,r}(t) &= C\, \tilde{x}_{i,r}(t)\,, \end{aligned} \tag{80}$$

where $X_{i,\hat{r}}(t)$ is comprised of components with the order lower than $|r|$, that is,

$$X_{i,\hat{r}}(t) = \left[\tilde{x}_{p_i,\hat{r}}^{\mathrm{T}}(t - \xi_{i,p_i}), \ldots, \tilde{x}_{i-1,\hat{r}}^{\mathrm{T}}(t - \xi_{i,i-1}), \tilde{x}_{i,\hat{r}}^{\mathrm{T}}(t - \xi_{i,p_i}), \ldots, \tilde{x}_{i,\hat{r}}^{\mathrm{T}}(t - \xi_{i,i-1})\right]^{\mathrm{T}} \tag{81}$$

for all possible $\hat{r}$-s that satisfy $|\hat{r}| < |r|$, while $f_{i,r}(X_{i,\hat{r}}(t))$ can be obtained from (77) and satisfies

$$f_{i,o}\left(X_{i,\hat{r}}(t)\right) \equiv 0\,, \quad f_{i,r}\,(0) = 0\,, \tag{82}$$

DOI: 10.1002/rnc

for all r-s where we define o as a zero vector that has the same dimension as r (cf. (78)). Note that the functions $f_{i,r}(X)$ vary for different r-s and may not have a general expression. Here, we only use its property (82).

Typically, larger M and R in (78) and (79) can improve the approximation accuracy, but they also increase the computation complexity. Here, we consider $M = 3$ and $R = 1$ such that (79) becomes

$$\tilde{x}_i(t,\epsilon) = \tilde{x}_{i,o}(t) + \epsilon_2 \tilde{x}_{i,[1,0]}(t) + \epsilon_3 \tilde{x}_{i,[0,1]}(t)\,, \tag{83}$$

for $i = 0, 1, \ldots, n$ where indeed o = [0,0]. For agent 0, considering (33), we have

$$\tilde{x}_{0,o}(t) = \begin{bmatrix} v_{\text{amp}} \sin(\omega t)/\omega \\ v_{\text{amp}} \cos(\omega t) \end{bmatrix}, \quad \tilde{x}_{0,[1,0]}(t) = \tilde{x}_{0,[0,1]}(t) \equiv \begin{bmatrix} 0 \\ 0 \end{bmatrix}. \tag{84}$$

Substituting (84) into (76) and (77) yields

$$\begin{aligned} f_{i,[1,0]}\left(X_{i,o}(t)\right) &= \sum_{j=p_i}^{i-1} \alpha_{i,j} \left(\frac{\tilde{s}_{j,o}(t-\xi_{i,j}) - \tilde{s}_{i,o}(t-\xi_{i,j})}{i-j} \right)^2, \\ f_{i,[0,1]}\left(X_{i,o}(t)\right) &= \sum_{j=p_i}^{i-1} \alpha_{i,j} \left(\frac{\tilde{s}_{j,o}(t-\xi_{i,j}) - \tilde{s}_{i,o}(t-\xi_{i,j})}{i-j} \right)^3, \end{aligned} \tag{85}$$

for $i = 1, \ldots, n$, where

$$X_{i,o}(t) = \left[\tilde{x}_{p_i,o}^{\mathrm{T}}(t-\xi_{i,p_i}),\ \ldots,\ \tilde{x}_{i-1,o}^{\mathrm{T}}(t-\xi_{i,i-1}),\ \tilde{x}_{i,o}^{\mathrm{T}}(t-\xi_{i,p_i}),\ \ldots,\ \tilde{x}_{i,o}^{\mathrm{T}}(t-\xi_{i,i-1})\right]^{\mathrm{T}} \tag{86}$$

(cf. (81) and (82)).

For $r = o$, the network (80) becomes a linear time invariant (LTI) system with excitations that arise from the head agent, that is, $\tilde{x}_{0,o}(t)$ in (84), and propagate through all agents to the tail agent n. Thus, the corresponding steady state are in the form

$$\tilde{x}_{i,o}^{(\mathrm{s})} = \begin{bmatrix} a_{i,o} \\ c_{i,o} \end{bmatrix} \cos(\omega t) + \begin{bmatrix} b_{i,o} \\ d_{i,o} \end{bmatrix} \sin(\omega t)\,, \tag{87}$$

where the superscript (s) indicates the steady state, while $a_{i,o}, b_{i,o}, c_{i,o}, d_{i,o}$ are constant coefficients to be determined. For compactness, we define a coefficient vector

$$z_{i,o} = [a_{i,o},\ b_{i,o},\ c_{i,o},\ d_{i,o}]^{\mathrm{T}}\,. \tag{88}$$

Substituting (87) into (80) with $r = o = [0,0]$ and matching coefficients of $\cos(\omega t)$ and $\sin(\omega t)$, respectively, we obtain

$$z_{i,o} = \left(D(\omega)\right)^{-1} E_{i,o}\,, \tag{89}$$

where

$$\begin{aligned} D(\omega) &= \begin{bmatrix} \omega F & -I_2 \\ \sum_{j=p_i}^{i-1} \varphi_{i,j}^* G(\omega\xi_{i,j}) & \omega F + \sum_{j=p_i}^{i-1} \kappa_{i,j} G(\omega\xi_{i,j}) \end{bmatrix}, \\ E_{i,o} &= \sum_{j=p_i}^{i-1} B_{i,j}^* \otimes G(\omega\xi_{i,j}) z_{j,o}\,, \end{aligned} \tag{90}$$

while $\varphi_{i,j}^* = \varphi_{i,j}(h^*)$ is given in (22) and

$$F = \begin{bmatrix} 0 & 1 \\ -1 & 0 \end{bmatrix}, \quad G(\theta) = \begin{bmatrix} \cos(\theta) & -\sin(\theta) \\ \sin(\theta) & \cos(\theta) \end{bmatrix}. \tag{91}$$

DOI: 10.1002/rnc

Because $\tilde{x}_{0,[1,0]}(t) = \tilde{x}_{0,[0,1]}(t) \equiv 0$, the networks (80) with $r = [1,0]$ and $r = [0,1]$ become LTI systems with excitations only arising from $f_{i,[1,0]}$ and $f_{i,[0,1]}$ in (85), respectively. Note that $\tilde{x}^2_{j,o}(t)$ contains frequency 2ω, while $\tilde{x}^3_{j,o}(t)$ contains frequencies ω and 3ω (cf. (87)). Thus, the steady states of (80) for $r = [1,0]$ and $r = [0,1]$ take the form

$$\begin{aligned}
\tilde{x}^{(s)}_{i,[1,0]} &= \begin{bmatrix} a_{i,[1,0]} \\ c_{i,[1,0]} \end{bmatrix} \cos(2\omega t) + \begin{bmatrix} b_{i,[1,0]} \\ d_{i,[1,0]} \end{bmatrix} \sin(2\omega t)\,, \\
\tilde{x}^{(s)}_{i,[0,1]} &= \begin{bmatrix} a_{i,[0,1],1} \\ c_{i,[0,1],1} \end{bmatrix} \cos(\omega t) + \begin{bmatrix} b_{i,[0,1],1} \\ d_{i,[0,1],1} \end{bmatrix} \sin(\omega t) + \begin{bmatrix} a_{i,[0,1],3} \\ c_{i,[0,1],3} \end{bmatrix} \cos(3\omega t) + \begin{bmatrix} b_{i,[0,1],3} \\ d_{i,[0,1],3} \end{bmatrix} \sin(3\omega t)\,.
\end{aligned} \tag{92}$$

We define the coefficient vectors as

$$\begin{aligned}
z_{i,[1,0]} &= \left[a_{i,[1,0]},\ b_{i,[1,0]},\ c_{i,[1,0]},\ d_{i,[1,0]}\right]^{\mathrm{T}}\,, \\
z_{i,[0,1],1} &= \left[a_{i,[0,1],1},\ b_{i,[0,1],1},\ c_{i,[0,1],1},\ d_{i,[0,1],1}\right]^{\mathrm{T}}\,, \\
z_{i,[0,1],3} &= \left[a_{i,[0,1],3},\ b_{i,[0,1],3},\ c_{i,[0,1],3},\ d_{i,[0,1],3}\right]^{\mathrm{T}}\,.
\end{aligned} \tag{93}$$

Substituting (92) into (80) and (85) with $r = [1,0]$ and $r = [0,1]$, respectively, we obtain

$$\begin{aligned}
z_{i,[1,0]} &= (D(2\omega))^{-1} E_{i,[1,0]}\,, \\
z_{i,[0,1],1} &= (D(\omega))^{-1} E_{i,[0,1],1}\,, \\
z_{i,[0,1],3} &= (D(3\omega))^{-1} E_{i,[0,1],3}\,,
\end{aligned} \tag{94}$$

where the matrix D is given in (90) and

$$\begin{aligned}
E_{i,[1,0]} &= \sum_{j=p_i}^{i-1} B^*_{i,j} \otimes G(2\omega\xi_{i,j}) z_{j,[1,0]} + \frac{\alpha_{i,j}}{(i-j)^2} I^* \otimes G(2\omega\xi_{i,j}) J_j\,, \\
E_{i,[0,1],1} &= \sum_{j=p_i}^{i-1} B^*_{i,j} \otimes G(\omega\xi_{i,j}) z_{j,[0,1],1} + \frac{\alpha_{i,j}}{(i-j)^3} I^* \otimes G(\omega\xi_{i,j}) K_j\,, \\
E_{i,[0,1],3} &= \sum_{j=p_i}^{i-1} B^*_{i,j} \otimes G(3\omega\xi_{i,j}) z_{j,[0,1],3} + \frac{\alpha_{i,j}}{(i-j)^3} I^* \otimes G(3\omega\xi_{i,j}) L_j\,,
\end{aligned} \tag{95}$$

where

$$\begin{aligned}
I^* &= \begin{bmatrix} 0 & 0 \\ 0 & 1 \end{bmatrix}, \\
J_j &= \begin{bmatrix} 0 \\ 0 \\ \left((a_{j,o}-a_{i,o})^2 - (b_{j,o}-b_{i,o})^2\right)/2 \\ (a_{j,o}-a_{i,o})(b_{j,o}-b_{i,o}) \end{bmatrix}, \\
K_j &= \begin{bmatrix} 0 \\ 0 \\ \left(3(a_{j,o}-a_{i,o})^3 + 3(a_{j,o}-a_{i,o})(b_{j,o}-b_{i,o})^2\right)/4 \\ \left(3(a_{j,o}-a_{i,o})^2(b_{j,o}-b_{i,o}) + 3(b_{j,o}-b_{i,o})^3\right)/4 \end{bmatrix}, \\
L_j &= \begin{bmatrix} 0 \\ 0 \\ \left((a_{j,o}-a_{i,o})^3 - 3(a_{j,o}-a_{i,o})(b_{j,o}-b_{i,o})^2\right)/4 \\ \left(3(a_{j,o}-a_{i,o})^2(b_{j,o}-b_{i,o}) - (b_{j,o}-b_{i,o})^3\right)/4 \end{bmatrix}.
\end{aligned} \tag{96}$$

DOI: 10.1002/rnc

Then, one can use (83), (87) and (92) to approximate the steady states of all agents sequentially from 1 to n.

APPENDIX E: PROOF OF THEOREM 5

Here, we still use the model (80). If the eventual disturbance attenuation (16) can be achieved in (80) for $M \to \infty$ and $R \to \infty$, then the nonlinear chain is capable of attenuating disturbances as the chain size increases to infinity.

As defined in Appendix D, the zero vector o has the same dimension with r. When $r = o$, the Laplace transform of (80) with zero initial condition becomes

$$\tilde{Y}_{i,o}(s) = \sum_{j=p_i}^{i-1} T_{i,j}(s, h^*)\tilde{Y}_{j,o}(s) \tag{97}$$

(cf. (82)), where $\tilde{Y}_{i,o}(s)$ is the Laplace transform of $\tilde{y}_{i,o}(t)$ and $T_{i,j}(s, h^*)$ is the link transfer function given in (38). Using the 'determinant-like' method presented in Section 4.2, one can calculate the head-to-tail transfer function between the steady-state outputs of agent 0 and agent n, which is given by $\tilde{Y}_{n,o}(s) = G_{n,0}(s, h^*)\tilde{Y}_{0,o}(s)$. Then, we cascade the network by k blocks, where agent kn is at the tail. It follows that the transfer function between the head agent 0 and the tail agent kn becomes

$$\tilde{Y}_{kn,o}(s) = G^k_{n,0}(s, h^*)\tilde{Y}_{0,o}(s)\,. \tag{98}$$

If the condition (44) holds, at the limit $k \to \infty$, we have $|G_{n,0}(\mathrm{j}\omega, h^*)|^k = 0$ and thus $|Y_{kn,o}(\mathrm{j}\omega)| = 0$ for all $\omega > 0$. Considering $\tilde{X}_{kn,o}(s) = E(s)\tilde{Y}_{kn,o}(s)$ where $E(s)$ is defined in (39), we have

$$\left\|\tilde{X}_{kn,o}(\mathrm{j}\omega)\right\| = \left\|E(\mathrm{j}\omega)\tilde{Y}_{kn,o}(\mathrm{j}\omega)\right\| \leqslant \|E(\mathrm{j}\omega)\|\left|\tilde{Y}_{kn,o}(\mathrm{j}\omega)\right| = 0\,, \tag{99}$$

for all $\omega > 0$, which implies that the steady state is zero, that is, $\tilde{x}^{(\mathrm{s})}_{kn,o}(t) \equiv 0$ with the superscript (s) denoting the steady state. Then, for agent kn, we assume the components of the steady state $\tilde{x}^{(\mathrm{s})}_{kn,\hat{r}}(t) \equiv 0$ for all $|\hat{r}| < |r|$ and investigate $\tilde{x}^{(\mathrm{s})}_{kn,r}(t)$. At the order $|r|$, substituting $\tilde{x}^{(\mathrm{s})}_{kn,\hat{r}}(t) \equiv 0$ in (80) while considering (82) also leads to an LTI system, which is the same as the system (80) with $r = o$. Based on the aforementioned analysis for the components of order $r = o$, one can show that $\tilde{x}^{(\mathrm{s})}_{kn,r}(t) \equiv 0$.

So far, we have shown that, at the limit $k \to \infty$, $\tilde{x}^{(\mathrm{s})}_{kn,o}(t) \equiv 0$ and $\tilde{x}^{(\mathrm{s})}_{kn,r}(t) \equiv 0$ if $\tilde{x}^{(\mathrm{s})}_{kn,\hat{r}}(t) \equiv 0$ for all $|\hat{r}| < |r|$. By induction, it follows that $x^{(\mathrm{s})}_{kn,r}(t) \equiv 0$ for all r-s. Substituting this into (79) implies $\tilde{x}_{kn}(t) \to 0$ as $t \to \infty$ and $k \to \infty$. Because this result is independent of the order of Taylor expansion, it holds when $M \to \infty$ and $R \to \infty$ in (78) and (79). Considering the property (43), we have that the values of ϵ_m are upper bounded for $m = 2, 3, \ldots$ and $\epsilon_m \to 0$ for $m \to \infty$. Therefore, if the components $\tilde{x}^{(\mathrm{s})}_{kn,r}(t) \equiv 0$ for all r-s, it follows that the steady state is $\tilde{x}^{(\mathrm{s})}_{kn} \equiv 0$ (cf. (79)).

ACKNOWLEDGEMENT

This study was supported by the National Science Foundation (award #1351456).

REFERENCES

1. Alon U. *An Introduction to Systems Biology: Design Principles of Biological Circuits*. CRC Press, Taylor & Francis Group: London, UK, 2007.
2. Olfati-Saber R, Jalalkamali P. Coupled distributed estimation and control for mobile sensor networks. *IEEE Transactions on Automatic Control* 2012; **57**(10):2609–2614.
3. Zhang L, Orosz G. Motif-based design for connected vehicle systems in presence of heterogeneous connectivity structures and time delays. *IEEE Transactions on Intelligent Transportation Systems* 2016; **17**(6):1638–1651.
4. Milanes V, Shladover SE, Spring J, Nowakowski C, Kawazoe H, Nakamura M. Cooperative adaptive cruise control in real traffic situations. *IEEE Transactions on Intelligent Transportation Systems* 2014; **15**(1):296–305.

DOI: 10.1002/rnc

5. Ge JI, Orosz G. Dynamics of connected vehicle systems with delayed acceleration feedback. *Transportation Research Part C* 2014; **46**:46–64.
6. Mesbahi M, Egerstedt M. *Graph Theoretic Methods in Multiagent Networks*. Princeton University Press, 2010.
7. Olfati-Saber R, Murray RM. Consensus problems in networks of agents with switching topology and time-delays. *IEEE Transactions on Automatic Control* 2004; **49**(9):1520–1533.
8. Xiao L, Boyd S. Fast linear iterations for distributed averaging. *Systems & Control Letters* 2004; **53**:65–78.
9. Liu ZX, Chen ZQ. Discarded consensus of network of agents with state constraint. *IEEE Transactions on Automatic Control* 2012; **57**(11):2869–2873.
10. Wang H. Consensus of networked mechanical systems with communication delays: a unified framework. *IEEE Transactions on Automatic Control* 2014; **59**(6):1571–1576.
11. Yu W, Chen G, Cao M. Consensus in directed networks of agents with nonlinear dynamics. *IEEE Transactions on Automatic Control* 2011; **56**(6):1436–1441.
12. Wen G, Duan Z, Yu W, Chen G. Consensus of multi-agent systems with nonlinear dynamics and sampled-data information: a delayed-input approach. *International Journal of Robust and Nonlinear Control* 2013; **23**.
13. Guo G, Ding L, Han QL. A distributed event-triggered transmission strategy for sampled-data consensus of multi-agent systems. *Automatica* 2014; **50**(5):1489–1496.
14. Orosz G, Wilson RE, Stépán G. Traffic jams: dynamics and control. *Philosophical Transactions of the Royal Society A* 2010; **368**(1928):4455–4479.
15. Jovanovic MR, Bamieh B. On the ill-posedness of certain vehicular platoon control problems. *IEEE Transactions on Automatic Control* 2005; **50**(9):1307C1321.
16. Oh KK, Moore KL, Ahn HS. Disturbance attenuation in consensus network of identical linear systems: an H_∞ approach. *IEEE Transactions on Automatic Control* 2014; **59**(8):2164–2169.
17. Lin P, Jia Y, Li L. Distributed robust H_∞ consensus control in directed networks of agents with time-delay. *Systems & Control Letters* 2008; **57**:643–653.
18. Swaroop D, Hedrick JK. String stability of interconnected systems. *IEEE Transactions on Automatic Control* 1996; **41**(3):349–357.
19. Rogge JA, Aeyels D. Vehicle platoons through ring coupling. *IEEE Transactions on Automatic Control* 2008; **53**(6):1370–1377.
20. Zhao Y, Minero P, Gupta V. On disturbance propagation in leader–follower systems with limited leader information. *Automatica* 2014; **50**:591–598.
21. Kianfar R, Augusto B, Ebadighajari A, Hakeem U, Nilsson J, Raza A, Tabar RS, Irukulapati NV, Englund C, Falcone P. *et al*. Design and experimental validation of a cooperative driving system in the grand cooperative driving challenge. *IEEE Transactions on Intelligent Transportation Systems* 2012; **13**(3):994–1007.
22. Geiger A, Lauer M, Moosmann F, Ranft B, Rapp H, Stiller C, Ziegler J. Team AnnieWAY's entry to the 2011 grand cooperative driving challenge. *IEEE Transactions on Intelligent Transportation Systems* 2012; **13**(3):1008–1017.
23. Guo G, Yue W. Autonomous platoon control allowing range-limited sensors. *IEEE Transactions on Vehicular Technology* 2012; **61**(7):2901–2912.
24. Guo G, Yue W. Sampled-data cooperative adaptive cruise control of vehicles with sensor failures. *IEEE Transactions on Intelligent Transportation Systems* 2014; **15**(6):2404–2418.
25. Gao W, Jiang ZP, Ozbay K. Adaptive optimal control of connected vehicles. *Proceedings of the 10th International Workshop on Robot Motion and Control*, Poznan, Poland, 2015; 288–293.
26. Orosz G, Moehlis J, Murray RM. Controlling biological networks by time-delayed signals. *Philosophical Transactions of the Royal Society A* 2010; **368**(1911):439–454.
27. Wilson D, Holt AB, Netoff TI, Moehlis J. Optimal entrainment of heterogeneous noisy neurons. *Frontiers in Neuroscience* 2015; **9**(192).
28. Ben-Israel A, Gilbert R. *Computer-supported Calculus*. Springer: New York, 2002.
29. Franzè G, Famularo D, Casavola A. Constrained nonlinear polynomial time-delay systems: a sum-of-squares approach to estimate the domain of attraction. *IEEE Transactions on Automatic Control* 2012; **57**(10):2673–2679.
30. Khalil HK. *Nonlinear Systems (3rd Edition)*. Prentice Hall: New Jersey, 2002.
31. Marinca V, Herisanu N. *Nonlinear Dynamical Systems in Engineering: Some Approximate Approaches*. Springer: New York, 2011.
32. Ulsoy AG, Peng H, Çakmakci M. *Automotive Control Systems*. Cambridge University Press: Cambridge, UK, 2012.
33. Orosz G. Connected cruise control: modeling, delay effects, and nonlinear behavior. *Vehicle System Dynamics* 2016; **54**(8):1147–1176.

DOI: 10.1002/rnc